Universidade do Minho

Escola de Ciências

Rodrigo Miranda e Cunha Cerqueira Marinho

Development of a microfluidic device for the isolation of ctDNA from the blood of cancer patients

October 2022

Development of a microfluidic device for the isolation of ctDNA from the blood of cancer patients

Rodrigo Miranda e Cunha Cerqueira Marinnho

UMinho | 2022

INTERNATIONAL IBERIAN NANOTECHNOLOGY LABORATORY

Universidade do Minho

Escola de Ciências

Rodrigo Miranda e Cunha Cerqueira Marinho

Development of a microfluidic device for the isolation of ctDNA from the blood of cancer patients

Master Thesis

Master in Biophysics and Bionanosystems

Work developed under the supervision of

Dra. Lorena Diéguez and

Prof. Dra. Ana Arminda Lopes Preto Almeida

October 2022

AGRADECIMENTOS

Às minhas orientadoras, Doutora Lorena Diéguez e Doutora Ana Arminda Lopes Preto Almeida, por toda a disponibilidade e apoio demonstrados ao longo do desenvolvimento deste projeto. À minha mãe, avós e restante família pela educação e incentivos e pela sua presença constante na minha vida. A todos os meus colegas de laboratório e amigos por me incentivarem a continuar, pela troca de ideias e tornarem este projeto possivel. E finalmente ao INL pela oportunidade, pela cedência do espaço, equipamentos e materiais necessários para a concretização deste projeto

DECLARAÇÃO DE INTEGRIDADE

Declaro ter atuado com integridade na elaboração do presente trabalho académico e confirmo que não recorri à prática de plágio nem a qualquer forma de utilização indevida ou falsificação de informações ou resultados em nenhuma das etapas conducente à sua elaboração.

Mais declaro que conheço e que respeitei o Código de Conduta Ética da Universidade do Minho.

Desenvolvimento de um dispositivo para o isolamento de ctDNA do sangue de pacientes com cancro

Resumo

O câncro da mama é um dos tipos de câncer mais comuns e uma das principais causas de mortalidade por câncer em mulheres[1]. A metástase é a causa básica da mortalidade relacionada ao câncer e, como o câncer é uma doença dinâmica e heterogênea, é crucial monitorizar a progressão da doença para combater a sua evolução[2]. Os métodos atualmente utilizados na clínica não são ideais, pois não representam o real estado do tumor. Para promover uma maior precisão na biomedicina a fim de melhorar o diagnóstico clínico e as decisões terapêuticas, é necessário desenvolver novas estratégias de detecção dos biomarcadores[3].

Por meio da biópsia líquida (LB), que é um método minimamente invasivo, é possível aceder informações sobre o tumor em tempo real, superando as limitações da biópsia solida[4], permitindo um diagnóstico mais preciso, precoce e uma terapia personalizada. LB analisa vários biomarcadores de câncer, incluindo ctDNA[5].

O DNA tumoral circulante (ctDNA) é um DNA fragmentado que se origina no tumor ou em células tumorais circulantes (CTCs) que circulam livremente no sangue do paciente, resultantes do fenômeno da metástase. Ao ser proveniente das células, é liberado após sua morte, por diferentes processos como apoptose, necrose e autofagia, assim o ctDNA apresenta menor uniformidade de tamanho e integridade quando relacionado ao DNA livre de células[6].

Estudos anteriores sobre o ctDNA mostraram que ele representa um biomarcador valioso para identificar mutações específicas que fornecem informações valiosas para o manejo clínico de pacientes com câncer, pois representa uma fonte em tempo real de informações relacionadas ao tumor, relevantes para a progressão do câncer e personalização do tratamento do paciente para melhorar a sua resposta. No entanto, as técnicas atuais de extração de ctDNA são complicadas e pouco eficientes[7–9].

Microfluídica é a área da ciência de manipulação e controlo de fluidos e partículas em microcanais[10]. Apresenta múltiplas vantagens no manuseio de amostras biológicas, como a possibilidade de dispositivos portáteis, descartáveis e de baixo custo, e a oferta de capacidade de integração para que toda a gama de protocolos laboratoriais de bancada, desde o manuseio de amostras até a reação, separação e deteção, possam ser incorporados e automatizados num único chip[11].

Palavras Chaves: Câcro da mama; CtDNA; Dispositivo; Metástase; Microfluídica;

Development of a microfluidic device for the isolation of ctDNA from the blood of cancer patients

Abstract

Breast cancer is one of the most common cancer types and a leading cause of cancer-related mortality in women[1]. Metastasis is the underlying cause of cancer-related mortality, and since cancer is a dynamic and heterogeneous disease, it is crucial to monitor disease progression to fight cancer evolution[2]. The methods currently used in the clinic, are not ideal as they fail to represent the real state of the tumor. To promote greater precision in biomedicine to improve clinical diagnosis and therapeutic decisions, it is necessary to develop new biomarker detection strategies[3].

Through liquid biopsy (LB), which is a minimally invasive method, it is possible to access information about the tumor in real-time, overcoming the limitations of tissue biopsy[4], and allowing a more precise and early diagnosis and personalized therapy. LB analyses several cancer biomarkers, including ctDNA[5].

Circulating tumor DNA (ctDNA) is fragmented DNA that originates in the tumor or in circulating tumor cells (CTCs) circulating freely in the patient's blood, resulting from the phenomenon of metastasis. When coming from cells, it is released upon their death, by different processes such as apoptosis, necrosis, and autophagy, thus ctDNA exhibits less uniformity in size and integrity when related to cell-free DNA[6].

Previous ctDNA studies have shown that it represents a valuable biomarker to identify specific mutations that provide valuable information for the clinical management of cancer patients as it represents a real-time source of tumor-related information, relevant to cancer progression and personalize patient treatment to improve their response. However, current techniques for ctDNA extraction are complicated and not very efficient[7–9].

Microfluidics is the area of science of handling and controlling fluids and particles in microchannels[10]. It presents multiple advantages to handling biological samples, such as the possibility of portable, disposable, and inexpensive devices, and the offer of integration capability so that the entire range of benchtop laboratory protocols, from sample handling to reaction, separation, and detection, can be incorporated and automated on a single chip[11].

Key Words: Breast Cancer; CtDNA; Device; Metastasis; Microfluidic;

Index

List of Images

List of Tables

List of Abbreviations

DCIS - ductal carcinoma in situ

LCIS - lobular carcinoma in situ

IDC - Invasive Ductal Carcinoma

ILC - Invasive Lobular Carcinoma

ER - estrogen receptor

PR - progesterone receptor

HER2 - human epidermal growth factor 2

HR - Hormonal receptor

TNBC - Triple-negative breast cancer

MRI - magnetic resonance imaging

CT - computerized tomography

CTCs - circulating tumor cells

LB - liquid biopsy

PCR - Polymerase Chain Reaction

ARMS - Scorpion Amplification Refractory Mutation System

NGS - Next Generation Sequencing

ctDNA - Circulating tumor DNA

cfDNA - cell free DNA

EGFR - epidermal growth factor receptor

mSPE - solid phase microscale extraction

SPE - solid phase extraction

PECVD - plasma enhanced chemical vapor deposition

HDMS - hexamethyldisilazane

DWL - Direct write laser

UV - ultra violet

RIE - reactive ion etching

ICP - inductively coupled plasma

PAG - photoacid generator

PDMS - Polydimethylsiloxane

EtOH - Ethanol

RF - radio-frequency

EVA - Ethyl-Vynil-Acetate

GPTMS - (3-glycidyloxypropyl)trimethoxysilane

MES - 2-(N-morpholino)ethanesulfonic acid

EDTA - Ethylenediaminetetraacetic acid

bp - base pares

HS - High Sensitivity

BR - Broad Range

SDNA - Salmon DNA

1 - Introduction

1.1 - Breast Cancer

In 2020 close to 19.292.789 new cases of cancer were identified worldwide [1]. This disease is also one of the deadliest, killing around 9.958.133 patients over the world, mainly due to the metastasis process[12]. Currently, there is already a high concern in cancer research, which allows the development of new treatment, detection, and prevention techniques. There are different types of cancer depending on where they originated[2]. This set of diseases is known for the abnormal development of cells, having different causes. This abnormal development begins with uncontrolled multiplication and the occurrence of abnormalities in the DNA of these cells. Since these cells are very similar to the cells of the adjacent organism, it is very difficult for them to be detected and to be a target for specific treatments, making their treatment very difficult and often harmful to the adjacent normal cells[13]. In this work, the main focus will be on breast cancer.

Despite all efforts, there is still no completely safe and effective treatment and the current ones still have unpleasant side effects, so it is necessary to develop techniques to increase efficiency and reduce collateral damage[3].

One of the most common cancers in women worldwide is breast cancer. The distribution of breast cancer is higher in developed countries compared to countries in development, on the other end, the survivability in developing countries is lower. There is also a huge concentration of cases in the age group of 50-69 years with nearly 49% of patients[1,14]. In 2020 breast cancer was the one with the most incidence having 11,7% of all cancer patients corresponding to 2.261.419 patients of both sexes and all ages, but all the cases were observed in women (Figure 1) [12]. This cancer type is also one with the highest mortality as many as 684.996 deaths in 2020, being cancer with the most deaths in women with a percentage of 15,5% of all cancer deaths (Figure 2)[12].

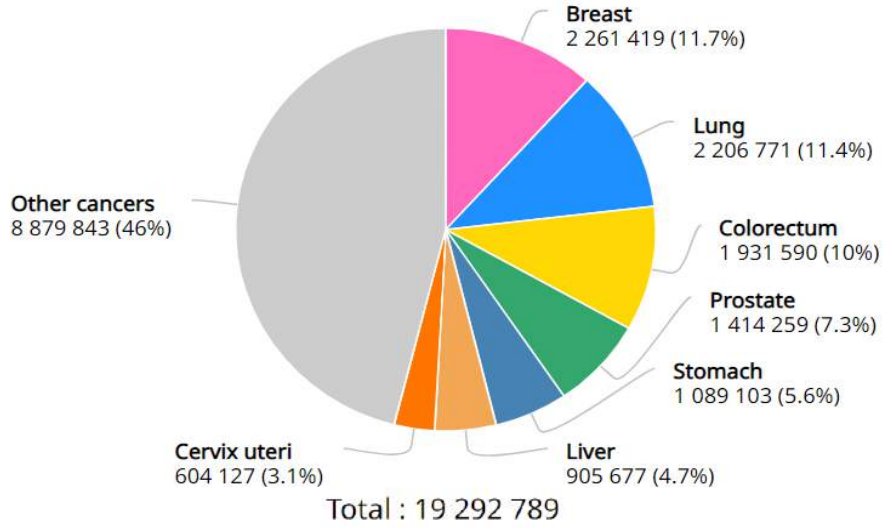

Figure 1 - Estimated number of cases in 2020 in the world for both sexes and all ages from all cancer types[12].

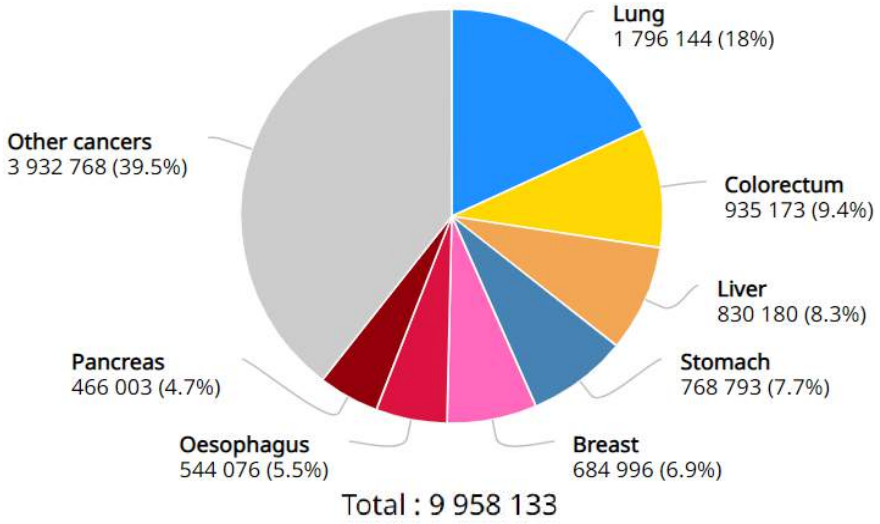

Figure 2 - Estimated number of deaths in 2020 in the world for both sexes and all ages from all cancer types[12].

1.1.1 – Early breast cancer

Breast cancer progress is divided into four different stages. The stages of cancer indicate the size of the tumor of abnormal cells and whether or not the tumor has spread to the blood. Stages 0 and I are the early stages of breast cancer the tumor has not spread and is still within the milk ducts of the breast having a small size and being highly treatable, the 5-year relative survival rate is 100%[15]. Stage II is when the tumor is starting to grow, and it may have expanded to the nearby lymph nodes, requiring more aggressive treatment[16]. Stage III is characterized by the tumor invading nearby lymph nodes and muscles,

not getting too far from the main focus point. Finally, stage IV is the last and more advanced one, at this point, the breast cancer has spread to other areas of the body, such as the brain, bones, lungs, and liver. This is a more problematic stage and has a lot of complications for the patient[17].

Early (or localized) breast cancer is characterized by not being extended away from the lobule or ducts where it originated (Figure 3)[18]. Carcinoma in situ is an early-stage, noninvasive, proliferation of epithelial cells that are confined to the ducts and lobules, by the basement membrane. That said there are two main types of non-invasive cancer depending on where they are formed, ductal carcinoma in situ (DCIS), the most predominant one, and lobular carcinoma in situ (LCIS). This first one is as the name suggests formed in the milk ducts. It is also the most common type of non-invasive breast cancer[19].

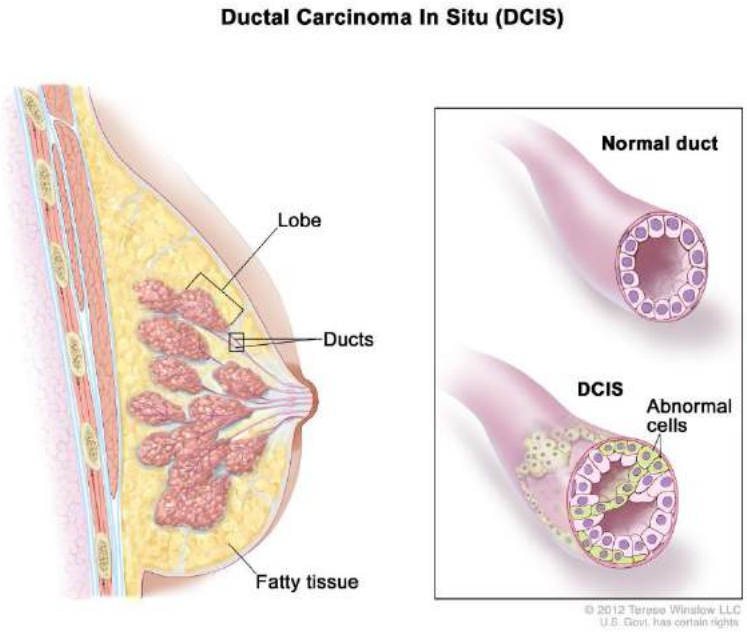

Figure 3 - Ductal carcinoma in situ (DCIS) and Abnormal cells found in the lining of a breast duct (Winslow, 2012).

Ductal carcinoma in situ (DCIS) is thought to be a precursor of most cases of invasive breast cancer and is characterized by the regional proliferation of malignant cells within the mammary lumens without invasion of the basement membrane[20,21], it occurs predominantly in women but can also occur in men. This type of pre-invasive lesion does not invariably progress to invasive malignancy. The second one, lobular carcinoma in situ (LCIS), originates from the terminal duct-lobular units and usually does not extend to the exterior.

Unlike DCIS, LCIS has a uniform appearance preserving the lobular structure. The loss of the tumor-suppressive adhesion protein E-cadherin promotes a non-cohesive cluster growth of the cells. This protein is responsible to mediate the contact inhibition of proliferation when cells reach confluence[22]. With this in mind, there is still a risk of developing invasive cancer from LCIS, and the molecular changes that are required for this evolution are poorly understood, so this type of non-invasive cancer is not considered a predecessor for the successive growth of invasive cancer, therefore an aggressive treatment is avoidable and only sequential follow-up is suggested[23].

1.1.2 - Metastatic breast cancer

If not controlled, early on, non-invasive cancer can turn into an invasive one. The invasive form of breast cancer is more predominant in women with 55 or older. This type of cancer can spread to other parts of the human body, passing to a metastatic phase. Based on the location, the tissue, and the cell types involved, invasive cancer can be divided into two types, just like non-invasive cancer. Invasive Ductal Carcinoma (IDC) is the most common type. Invasive Lobular Carcinoma (ILC) is the other most common type, which generally affects older women[24].

Metastatic breast cancer, or stage IV, are late-stage breast cancers that have spread to other parts of the body, most commonly the bones, lungs, brain, and liver, and can also be in lymph nodes and the armpit. Because of the metastatic process, breast cancer can reappear on different parts of the body months or years after the first diagnosis, this is called metastatic recurrence or distant recurrence, but it's not yet clearly understood because of its variability, which differs from person to person, depends on the unique molecular biology of the tumor and the stage at the time of the first diagnosis. Close to 30% of women diagnosed with early-stage breast cancer develop metastatic breast cancer. It's not clear how many cases of breast cancer metastasize in men because of its reduced amount, but men are also diagnosed with metastatic breast cancer[24–26].

As Metastatic breast cancer is not the same for everyone who has it cancer the survivability is variable as well, at this stage the cancer is not curable but with the right treatment can be controlled for some years. The 5-years survival rate after diagnosis for people with stage IV breast cancer is 26.5%[17,27].

1.1.3 - Molecular subtypes

Gene expression studies have identified several distinct breast cancer subtypes that differ significantly in prognosis as well as in the therapeutic targets present in the cancer cells. The advances

in gene expression techniques helped to characterize the main clinical parameters and pathological markers that make possible the differentiation between the different subtypes of breast cancer. This list of intrinsic genes is constituted by several cluster genes related to estrogen receptor (ER) expression, progesterone receptor (PR) expression, human epidermal growth factor 2 (HER2) expression, proliferation, and basal cluster [24]. Those markers are currently used in the clinic to identify the possible subtype of cancer, and that understanding allows a division of cancer into 4 main molecular or intrinsic subtypes that are based on the expression pattern of those genes[28].

Hormonal receptor (HR) –positive breast cancer is mainly composed of two different types, Luminal A and Luminal B. Those types of cancer are characterized by being ER and PR-positive [29]. Luminal A breast cancer is the most common molecular or intrinsic subtype of breast cancer that grows normally at a slower rate than the other cancer types. This type of cancer is normally called HR-positive, using estrogen and progesterone as primary growth factors. This cancer subtype is also a HER2-negative. Drugs that lower the amount of estrogen and progesterone tend to be useful in treating this type of breast cancer, that said the treatment for this subtype of cancer normally involves hormonal therapy [28].

Luminal B tends to grow faster than luminal A and is less common[28]. In opposition to luminal A, this type of cancer is positive for both ER/PR and HER2. As such it's more aggressive and more difficult to treat. This is also supposed to be more predominant in a younger group of the population [30,31].

Approximately 20% of all invasive cancers are HER2-positive, which makes this a very common subtype of cancer. HER2 receptors, produced by HER2 gene sequencing, control how healthy breast cell grows, divides and repairs themselves[32]. HER2-positive breast cancer cells carry too many copies of the HER2 gene making the cells divide and grow rapidly and without control. HER2-enriched breast cancer, this type of cancer is not positive for ER and PR, being only positive for HER2. It grows faster than the previous two and is generally more aggressive, having the worst prognosis. However, depending on cancer's state, this can be treated by combinations of breast cancer surgery, radiation therapy, chemotherapy, and/or administration of targeted therapy such as the immune monoclonal antibody, trastuzumab, Perjeta, Tykerb, and kadcyla[24,32,33].

Triple-negative breast cancer (TNBC) is a type of breast cancer with negative expression of ER, PR, and HER2. This type of breast cancer is usually invasive, more aggressive, and usually begins in the breast ducts. In women with TNBC, as the cells do not have any receptors, the treatment cannot be done based on hormonal therapy, it must be treated with more aggressive therapies like chemotherapy, radiation therapy, and non-HER2 targeted therapy. TNBC occurs mostly in young women under 40 years

old, making up approximately 15 to 20% of all breast cancer patients. Compared with other subtypes of breast cancer, TNBC is highly invasive, metastasizing in approximately 45% of the cases, normally spreading to the brain and visceral organs. The survivability for this subtype of cancer is short and the mortality rate is 40% within the first 5 years after diagnosis, for metastasized patients is only approximately 13 months[34,35].

1.1.4 - Current diagnostic and monitoring tools and treatment selection

Thanks to the rapid progress in molecular biology, systems biology, genome sciences, and nanotechnology in the past decades, we are now able to understand cancer a little bit more at different levels, cellular, molecular, and genomic[24]. Currently, numerous cancer diagnostics and treatments have been developed and used. Different types of ways to avoid cancer are being developed, for example, therapy with antiestrogens such as raloxifene or tamoxifen might avoid cancer in individuals with a higher risk of developing it[36,37]. The use of nanoparticles and/or nanomaterials increased the efficiency in the delivery of anticancer drugs, which allowed to facilitate rapid advances in nanomedicine[38].

It is important to get the necessary information before starting any treatment, for that, there is a variety of different cancer diagnostics that can be made in the clinic. This will help support the decision on which tools will be used. Examples of those diagnostics are:

Brest exam is a simple exam done by the patient or the doctor by checking specific areas on the breasts and lymph nodes around the armpit, expecting lumps or other abnormalities[39].

A mammogram is an exam made using an X-Ray machine, if an abnormality is detected on a screening mammogram, a diagnostic mammogram is recommended to further evaluate the abnormality. This is considered one of the best clinical early diagnostics, even though some cancer is not detected by this method and the sensitivity of mammography is affected by dense breast tissue[40,41].

Ultrasonography uses high-frequency sound waves to screen and get images of structures inside the breast, normally used to distinguish if breast lumps are a solid mass or a fluid-filled cyst. For the Early detection of breast cancer, It's still not as effective as mammography and has some obstacles[42,43].

A solid/tissue biopsy is a definitive way to obtain a final diagnosis of the tumor and its molecular subtype. It is performed using a specialized needle device guided by an X-ray or another imaging test to extract an important portion of tissue from the area supposed to be abnormal for further analysis. Despite being the standard method for cancer characterization the solid biopsy shows some limitations. The

principal one is that a single solid biopsy is not possible to observe tumor heterogeneity, being bound to the area where the biopsy was done, which can lead to an incorrect characterization of the tumor[44].

After cancer has been detected and identified several possible treatments may be planned to have the best possible results. Surgery to remove breast cancer has been the treatment of choice for breast cancer. This process has different approaches starting from only breast cancer, the lumpectomy, which is a breast-conserving surgery the tumor is removed alongside a small margin of surrounding healthy tissue. This treatment is more common on smaller tumors. The entirety of the breast can be removed by a process called mastectomy, normally none of the breast tissue is left but more recently some are being left to improve the final lock of the breast. Despite being the go-to for breast cancer treatment this surgery carries risks of pain, bleeding, infection, and arm swelling (lymphedema)[45].

Radiation therapy has been long used in breast cancer treatment, it uses high-powered beams of energy, such as X-rays, and portions to destroy cancer cells. This process is normally used after a lumpectomy. Breast cancer radiation therapy can last from three days to six weeks. Then again there are side effects to this type of treatment, for example, fatigue, swollen or more firm breast tissue, red rash on the local of the radiation target point, and more serious problems like damage to the earth, lungs, and other parts of the body[46].

Chemotherapy is a treatment based on the use of drugs to destroy cancer cells. This treatment is normally used on patients where cancer has already spread to other parts of the body, before surgery on patients with large breast tumors to shrink them down to a size where they can be removed, and after surgery, if there is a high risk of cancer returning. As always there are some side effects depending on the drug used, the most common are hair loss, nausea, vomiting, fatigue, and increased risk of developing an infection. Some rare side effects are infertility, premature menopause, nerve damage, damage to the earth and kidneys, and very rare cases of blood cell cancer[47].

Hormone-blocking therapy is targeted at hormone-based breast cancers, this therapy can be used before or after surgery or other treatments to decrease the chance of reoccurrence, if cancer has metastasized already hormonal therapy can help reduce and control the spread. This therapy has some rare side effects that include the risk of bone thinning and blood clots[48].

Targeted therapy drugs are a more modern approach to cancer treatment that is still being improved, but is very interesting since it is safer than the previous ones and can be more efficient. This

therapy uses targeted drugs for specific abnormalities, like proteins that some cancer cells overproduce the HER2[49].

Normally a combination between surgery and hormonal therapy, targeted therapy, chemotherapy, or radiotherapy, depending on the molecular subtype, the stage, and the aggressiveness. Afterward, once patients are cured and stable, they are monitored for the appearance of recurrence using imaging technologies.

Breast magnetic resonance imaging (MRI) is a non-invasive tumor detection tool with a reliable sensitivity, not as commonly used for early detection as the previous methods but is still solid for analysis before applying treatment planning. Being a safer method for the patient since does not use any type of radiation[50].

A computerized tomography (CT) scan is an X-ray technique that gives information about the internal organs of the body. Normally CT scans are not used regularly and are focused to detect if the tumor has moved into the chest wall. It may also be used on different parts of the body t where the tumor could spread[51].

Taking into account all the cancer problems already discussed, we emphasize its ability to metastasize, spreading to other regions of the body, making its treatment even more difficult. Therefore, enhancing breast cancer outcomes and survival by early detection remains the foundation of breast cancer regulations, consequently, the search for new diagnostic methods is of great interest[52].

1.2 – Liquid Biopsy

As shown before, the main cause of cancer-related death is distant metastases, which are still difficult to diagnose after solid tumor diagnosis and treatment. The current methods, by diagnosing the primary tumor alone, can sometimes give misleading information regarding the different characteristics of metastases, since cancer is a heterogeneous and dynamic disease that evolves with the pressure of treatment, and imaging technologies for patient monitoring are not sensitive enough to detect a metastatic lesion when it is still small and fail to update the molecular characteristics of the tumor[53]. A solid biopsy of the metastatic tumor is not always possible, due to the tumor location and the related patient discomfort. However, in 1869 a pathologist named Thomas Ashworth provided evidence for the presence of circulating tumor cells (CTCs) in the blood of a metastatic cancer patient. The study of those biomarkers is known as liquid biopsy (LB). The concept of LB aims at simple, fast, and cost-efficient monitoring of

disease status or response to treatment. Compared to tissue biopsies, LB may offer a more comprehensive cross-section of heterogeneous diseases. The LB complements personalized medicine[54].

This method provides several advantages over solid tumor biopsy, which is the current gold standard method, has been said previously it is less invasive, dangerous, and painful, and it provides a more representative characterization of the tumor genetics and allows to get a real-time follow-up of the tumor allowing for more precise responses and treatments for the cancer patient. The process to make this possible cannot be done in only one single biopsy but at the same time, it's easier to obtain repeated blood samples over time[5,55].

1.2.1 - Circulating biomarkers

LB is a minimally invasive tool to utilize tumor biomarkers in body fluids like blood, urine, stool, saliva, pleural fluid, peritoneal fluid, and cerebral spinal fluid[56]. These biomarkers can be circulating tumor cells (CTCs), small fragments of DNA and RNA from the tumor cells, circulating protein and metabolites, platelet RNA, and extracellular vesicles like exosomes and microvesicles[57]. Some of the most used biomarkers are CTCs which are complete cells derived from the tumor that can be captured in a single blood draw. Among other challenges, CTC capture is hard due to its rarity in the blood of the patient, nevertheless, a single CTC can provide a lot o information about the tumor[58]. Other similar biomarkers are the extracellular vesicles, which get expelled by tumor cells, these biomarkers can have a range of sizes from tens to hundreds of nanometers. They carry a lot of proteins and nucleic acids that can provide a hand full of information about the tumor, they are suspected to be responsible for cell signaling[59]. Another biomarker that is starting to be widely used is the ctDNA as an important font of information about the tumor, being able to identify the mutation and specific alterations in the course of the treatment phase permitting the adaptation of those treatments for more specific focused ones[60]. Resulting in being the biomarker the focus of this work.

1.2.2 - Relevance of ctDNA, approved diagnostic tools

Of all the different biomarkers that can be used by LB, the main one focused in this work is the circulating tumor DNA[5,55]. The main challenge of LB on the Circulating tumor DNA spectrum is to detect a wide range of fragmented sizes, as well as the correct choice of diagnosis for each type of cancer[61]. To try and solve that challenge different technologies have been developed including Polymerase Chain Reaction (PCR), Scorpion Amplification Refractory Mutation System (ARMS), beads, amplification,

magnetic analysis, emulsions, and Next Generation Sequencing (NGS)[62,63]. These technologies are important factors in clinical decisions, diagnostics, and prognostics for cancer treatments[64].

Circulating tumor DNA (ctDNA) is fragmented DNA derived from tumor cells that freely circulate in the patient's blood (Figure 4)[76]. This DNA should not be confused with the free DNA of normal cells (cfDNA). CtDNA proves to be very important as it can provide the complete genome of the tumor, allowing monitoring in the form of blood collection throughout the treatment regimen[65].

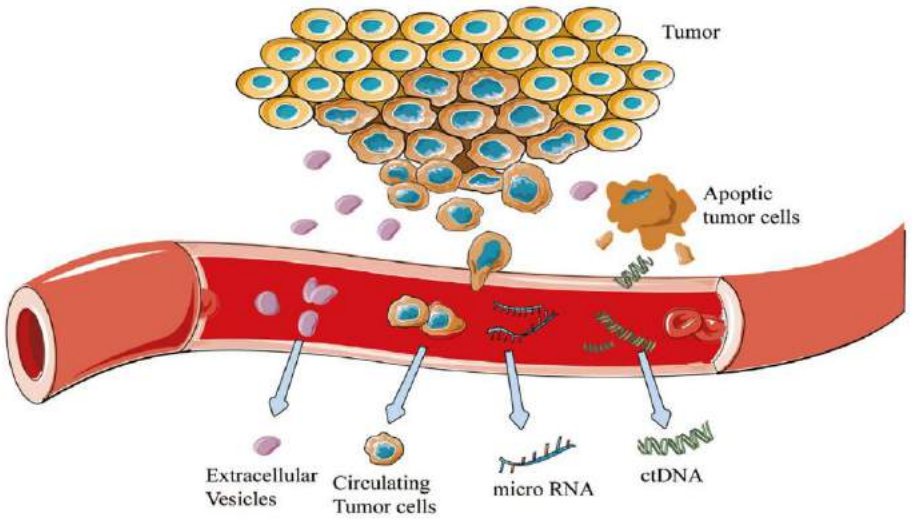

Figure 4 – Representatrion of diferent circulating biomarkers in the blood of a cancer patient[76].

CtDNA originates in the tumor or in circulating tumor cells (CTCs), resulting from the phenomenon of metastasis. When coming from cells, it is released upon their death, by different processes such as apoptosis, necrosis, and autophagy, thus ctDNA exhibits less uniformity in size and integrity when related to cfDNA, having a mean length of around 150 bp[55]. It's found in circulation in percentages from 3 % to 93 %, this variation can indicate the tumor stage, with an increase in the percentage of ctDNA with the increase of the tumor. According to studies, these fluctuating results for quantity, form, and integrity may have resulted in different isolation methods and the sources of the samples tested[6].

The latest studies and advances in DNA sequencing techniques and understanding of the molecular biology of tumors have promoted the use of ctDNA as a tool for the early detection of cancer, allowing for better treatments, by allowing for rapid intervention in the early stages of the disease[7].

We can now understand the importance of using ctDNA for early detection or during treatment, in real-time and in a non-evasive way, of the specific information related to the tumor and its evolution. It may have utility in the adjuvant therapeutic setting, allowing the identification of patients at high risk of disease recurrence based on the detection of post-surgical minimal (or molecular) residual disease (MRD). Since ctDNA has the heterogenetic characteristics of tumors and is possible to detect mutations and alterations in the circulating tumor DNA, which can provide us with even more information about the progress and development of the tumor, it has been considered a dynamic biomarker with the potential for diagnostic, predictive, and prognostic applications for various types of solid tumors[66].

The relevance of ctDNA has been widely proved in the clinic with the introduction of companion diagnostic tools like the COBAS test to detect epidermal growth factor receptor (EGFR) mutations in lung cancer. For example, ctDNA in breast cancer has moved from purely fundamental research to nearby daily use for treatment selection and drug-resistance assessment[66]. However, the isolation and enrichment of ctDNA is a major challenge, given its low concentration in the bloodstream and the high degree of cfDNA fragmentation. Therefore, consistent and reproducible sampling factors described in the following sections are essential to obtain superior quality results in the pre-analytical stage[10].

1.2.3 - Current tools for extraction and analysis

As the importance and interest in ctDNA increased, the necessity to isolate and separate it from the blood of patients has increased as well. Since the quality of the analysis and the sequencing data depends on the quality of the techniques used, different techniques have been developed and improved to perform a good analysis[67]. In succession to that evolution, a group of commercial kits was developed that uses a real-time PCR-based system. Examples of these kits are the QIAamp circulating nucleic acid kit (QIA), the PME free-circulating DNA Extraction Kit (PME), the Maxwell RSC ccfDNA Plasma Kit (RSC), EpiQuick Circulating Cell-Free DNA Isolation Kit (EQ), and the NEXTprep-Mag cfDNA Isolation Kit ($NpM_{V1/2}$). Those kits were compared on a different project where the QIA kit processed a volume of 1 ml of plasma with an elution volume of 100 µl, and the rest of the kits processed a volume of 0,1 ml of plasma with an elution volume of 50 µl, with the NpM($NpM_{V1/2}$) kits having an elution volume of 20 and 12 µl respectively, all samples were quantified using Qubit dsDNA Has assay kit. All the protocols for the kits were manual or had some manual steps like the QIA kit, except for the RSC kit the protocol was fully automated. The kits had a good recovery rate of approximately 50% to ctDNA[68].

DNA purification and concentration are crucial steps in any DNA-based analytical system. During this step, a high concentration of high-quality DNA must be obtained so that the following steps are more likely to be successful. Despite this importance, this step is not always taken with the greatest concern, making the final results not as expected. To this end, in recent years, several miniaturized devices and different protocols have been developed to allow for the purification and pre-concentration of DNA[69].

Purification and preconcentration of DNA are often achieved by solid phase microscale extraction (mSPE). An mSPE-based protocol typically consists of three distinct steps, first a binding step in which the DNA present in the liquid will be immobilized in the solid phase, a second washing step in which unbound molecules are removed using a different buffer and finally an elution step in which the purified DNA will be recovered from the solid support to the liquid using a low salt buffer. Other approaches based on solid phase extraction (SPE) can benefit from the miniaturization of devices due to the increased surface area-to-volume ratio. These approaches allow highly efficient DNA purification and concentration of complex samples and samples with minimal DNA content, allowing the detection of target DNA in the following analysis steps[70,71].

1.2.4 - Limitations of current extraction tools

Even with good recovery rates, these types of kits still have some problems that can make them not viable ways to extract ctDNA from patient samples. Some of the problems fall into the price of the base kit and the experience required for the user to have to use them properly. Despite that there is some variability in the results among laboratories, this again probably has to do with the way the operator uses the kit[72].

1.4 - Microfluidic

1.4.1 - Benefits of Microfluidics

Microfluidic is a technical field that studies and controls the behavior of fluids and particles when they flow through microscale channels. A microfluidic chip is an array of microchannels molded into a material such as glass, silicon, etc. These channels are connected to achieve the required results. Microfluidics experienced rapid growth in the 1990s when analytical chemistry techniques and microscale

technologies were gaining in popularity and recognition[11]. Microfluidics is a platform technology that allows the automation and multiplexing of laboratory equipment, drug screening technologies, and in vitro diagnostic devices[73]. Although there are several possible applications for microfluidics, given its potential to significantly reduce sample volumes, and perform reactions, separations, and detections quickly, sensitively, and inexpensively, the main reason for the rapid evolution of microfluidics is its potential for biological applications (Figure 5), such as drug screening, biosensors, diagnostics, analysis, and cell manipulation, among others. Furthermore, these devices for the biological application are cheaper than most competing techniques, increasing their use for testing and research[11,73,74].

The use of more appropriate techniques with characteristic length scales proportionally to the dimensions of the target to be studied, such as cells and molecules among others, as shown in figure 5, microfluidics techniques have a good range of possible scales for evaluation, in comparison with other techniques commonly used in the laboratory[11].

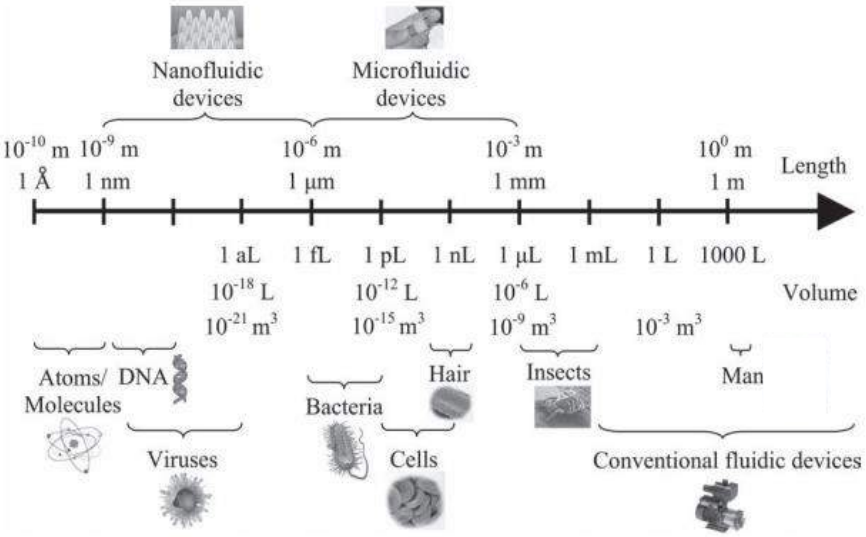

Figure 5 - Characteristic length scales of microfluidics systems in relation to the sizes of different biological entities.

Microfluidics also offers several other advantages over conventional laboratory-scale assays. The inverse characteristic length scale of the surface area to volume ratio implies that heat and mass transfer into or out of a chip can be increased as the device's dimensions are reduced; other interfacial physicochemical phenomena not commonly found in macroscopic dimensions can also be explored. On the other hand, microfluidics offers integration capability so that the entire range of benchtop laboratory protocols, from sample handling to reaction, separation, and detection, can be incorporated and

automated on a single chip in a manner, not unlike the operations units of a chemical plant. With advances in microfabrication and nanofabrication, large-scale economies can be capitalized on to make portable, disposable, and inexpensive devices that could potentially revolutionize medicine [11].

1.4.2 – Microfluidic in liquid biopsy

Microfluidics has been widely used to help the isolation of the biomarkers needed for liquid biopsy. Recent advances in microfluidics allow the capture of exomes and molecular detection with great selectivity and sensitivity[75]. The isolation of immunoaffinity-based exosomes can be done with microfluidic devices by manipulating affinity particles/magnetic beads or modifying microchannel surfaces with antibodies. In 2010, Chen et al. reported the first microfluidic exosome isolation platform, which used an anti-CD63 functionalized surface for the immunocapture of exosomes from human sera[76]. Kanwar et al. developed a platform called ExoChip, that utilized the same anti-CD63 functionalized surface circular microchamber to capture exosomes[77]. Zhao Z. et al. developed A Microfluidic ExoSearch Chip for Multiplexed Exosome Detection for Blood-Based Ovarian Cancer Diagnosis, the production of the chip used PDMS for inexpensive and fast production, and the process used immunomagnetic beads to capture the exosomes[78]. More examples of the importance of microfluidics devices are also represented by the isolation of CTCs existing already different methods for that. Examples of those are Microfiltration Separation Methods, Hydrodynamic Separation Methods, Dielectrophoretic Separation Methods, Surface Affinity Separation Methods, Immunomagnetic-Based Separation Methods, and a Summary of Biological-Based Separation Methods[79]. Those are some examples of the application of microfluidics on liquid biopsy apart from the ones that will be focused on next.

1.4.3 – Microfluidics for extraction of nucleic acids from complex matrices

Microfluidic technology is a powerful tool for miniaturization, and its application in DNA-based techniques has grown exponentially. Despite the increased total integration of such devices, most still require prior sample preparation that includes cell lysis and DNA purification steps. Sample preparation is one of the biggest obstacles to the full integration of miniaturized DNA-based analysis, and is still a step behind when compared to other analytical steps. In the case studied in this work, due to the complexity of blood and the fact that it is necessary to separate two very similar types of DNA, fragmented and in

low quantity, it becomes a challenge to achieve a successful result, as in other types of samples as in food products and with high concentrations of contaminants and clinical samples [10,70].

Different projects develop different types of devices, and some of them were used as a reference for the ones produced in this project. These devices mostly helped with the design but not only, gave some hints to help on the protocol and on the material used to produce the new devices. The first device has silicon wafers anodically bonded to glass covers, with 10 μm square pillars etched in 20–50 μm deep silicon and 10 μm spacing between pillars. It uses flow rates that vary from 2 to 10 μl/min. In that project, the DNA was quantified using the PicoGreen reagent from Molecular Probes[80](Figure 6).

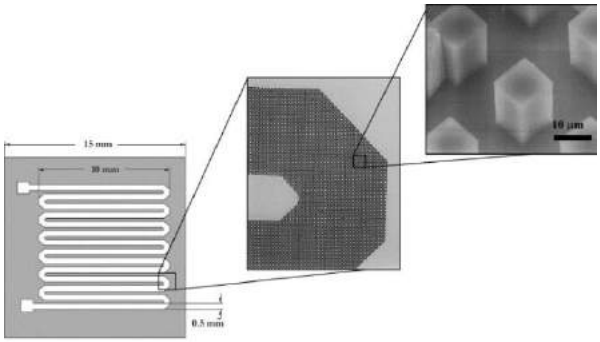

Figure 6 - Representation of the design of the microfluidic device and its pillars[80].

The next Device was used inside a bigger ship and was made from a Silicon wafer created using standard photolithographic techniques and deep reactive ion etching, oxidized to yield a 150 nm silica surface layer suitable for DNA capture, having 15 μm width pillars etched in 200 μm deep silicon and 30 μm center-to-center spacing between pillars. The protocol uses flow rates that vary from 1 to 100 μl/s. The recovery rates of DNA from the chip were typically between 10 and 25%[81] (Figure 7).

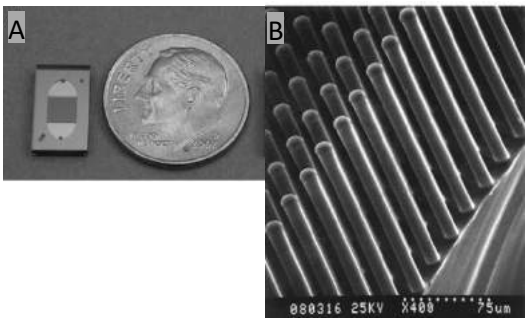

Figure 7 – (A) Representation and size of the microfluidic device, (B) Micro pillars distribution[81].

The next device has a more complex shape, with 64 channels for DNA extraction where each channel has 0.5 cm long by 17 µm deep, with a top width of 83 µm, and a width of 33 µm at the bottom (Figure 8). The coating process was obtained by incubation of the channel using 0,1% GPTMS, to act as a cross-linker to the channel wall, and 1% chitosan before rinsing with 10 mM acetic acid and water to remove unbound chitosan. The flow rate was fixed at 1,0 µL/min DNA was detected using PicoGreen intercalating dye in a TD-700 fluorometer. Before extraction, the microchip was cleaned using 10 mM Tris buffer (pH 9,0) pulled through the device, the microchip was then filled with 10 mM MES buffer (pH 5,0) to protonate amino groups on the chitosan-coated on the surface of the channels DNA sample in 10 mM MES buffer at pH 5,0 (loading buffer) was added to the inlet reservoir and flowed through the channels, for the washing step, 4 µL of 10 mM MES buffer pH 5,0 (washing buffer) was used to remove any unbound material from the channels. After washing the channels, 10 mM Tris buffer at pH 9,0 containing 50 mM KCl (elution buffer) was added to the reservoir and flowed through the channels to elute DNA. The DNA was detected using PicoGreen intercalating dye in a TD-700 fluorometer. The efficiency of this device is between 65% and 75% using Lambda DNA and human genomic DNA[82].

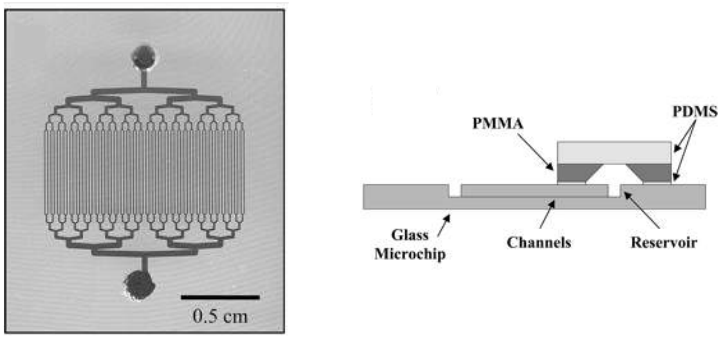

Figure 8 - Design and composition of the Microfluidic device[82].

The last relevant device is formed by a group of beds, each one 40 mm long and populated with 5,8 µm diamond-shaped pillars that were spaced by 6,9 µm with a height of 11,6 µm (Figure 9). The main process for this device was supported by the fact that neutralized charge of DNA due to the presence of salt in the immobilization buffer allowed for DNA to condense onto a negatively charged surface. The flow rates used varied from 1 to 2 µl/min. Quantitative PCR (qPCR) was used to assess the amount of DNA extracted. This device was used to purify cfDNA (122 and 290 bp). The best results showed a recovery rate above 90%[83].

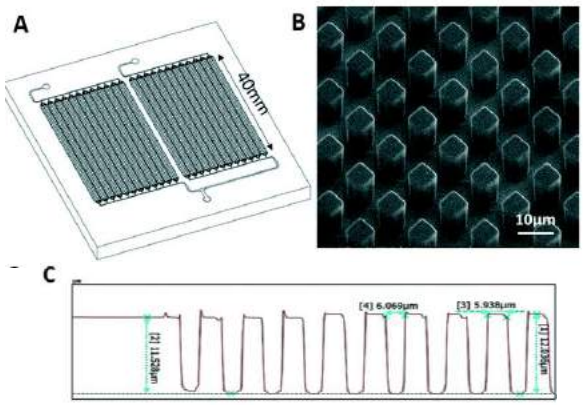

Figure 9 - (A) Schematic of the 24-bed device (B) SEM images of pillar arrays. (C) Profilometryanalysis of the device[83].

Of all the devices some were more interesting than others having more emphasis, better recovery rates faster flow rates, and an overall more interesting design (Table 1), influencing more on the creation of the design of this project's devices.

Table 1 - Comparison between the different devices studied for this project.

	Date	Dimensions	Flow Rate	Surface area	DNA type	Recovery (%)
1.	2003	Pillars (10/10/20-50)	2 to 10 µl/min	2.45 cm^2	Lambda DNA (500 bp)	55%
2.	2008	Pillars (15/15/200)	1 to 100 µl/s	4.2 cm^2	Bacillus anthracis genomic DNA	10-20%
3.	2006	64 V shaped Channels 50 mm long and 17 µm deep Top width of 83 µm, and 33 µm at the bottom	1.0 µL/min	Surface area-to-volume Rate of 151 mm^{-1}	Lambda DNA (50kbp) Human genomic DNA DNA from blood	70% 65% 75%
4.	2018	40 mm long Pillar beds Pillars (5.8/6.9/11.6)	1 to 2 µl/min	Per be: 1.22cm^2	cfDNA (122 and 290 bp)	90%

2 - Objectives

With advances in microfluidics and its use for real-time and non-evasive analysis of DNA, it has been increasingly used for the collection and detection of DNA under different conditions. This work is intended to use these advantages to promote greater precision in biomedicine to improve clinical diagnosis and therapeutic decisions, quickly and effectively detecting the presence of ctDNA in cancer patients, thus making possible a more in-depth study of the different characteristics of cancer in question. Therefore, the objective of this work is to develop a microfluidic tool to isolate ctDNA from whole blood, which is relevant for the early detection of cancer at the point of care, accurate prognosis, and

personalized treatment. The device will be functionalized with a positively charged compound, allowing electrostatic interactions with the DNA fragments. To analyze the efficiency of the module, known concentrations of DNA fragments will be spiked and extraction efficiency will be quantified using the Qubit Fluorometer system.

The specific objectives are the development of a microfluidic device using inexpensive materials permitting the replication of the device multiple times, in this case, PDMS bonded to glass slides. Create a unique design that will make possible the processing of 1 ml of sample. Utilize and optimize a protocol that makes use of the negative charge of the DNA to make it bond with the chitosan that will be revesting the walls of the device. Then after that the utilization of an elution buffer with a much higher pH so that is possible to break the chitosan-DNA bond and this way isolate the DNA.

3 - Material and methodology

3.1 – Device Production

3.1.1 – Design

After some research three designs were idealized using AutoCAD, AutoCAD is a 3D software used in the microfluidic environment to create a 2D layered drawing of the desired device (Figure 10).

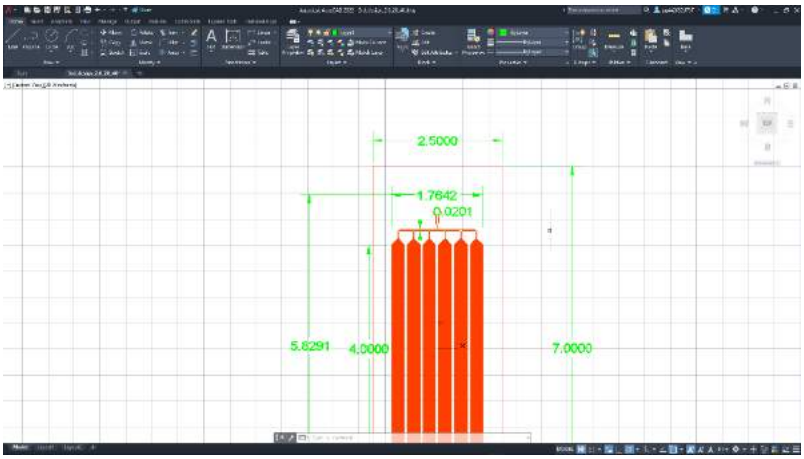

Figure 10 - Workspace using AutoCAD to develop the design of the devices used on this project.

The designs were divided into two groups, having a group with smaller devices and another group with a bigger device. The two devices in the first group followed the same base design as shown in Figure 11A and 11B, both designs have a length of 2,8 cm and a width of 1,27 cm. The small channels have a length of 1,7 cm and a width of 80 um. The main difference between them is in the disposition of the pillars inside the channels (figures 11).

Device A has a single pillar in the middle with a diameter of 40 µm and a semi-circle on the walls of the channels and a spacing between them of 13 µm for one side and 27 µm for the other (Figure 11A).

The device B has an array of 3 pillars diagonally spaced by 10 µm from one another, the pillars have a diameter of 20 µm, the last pillar is embedded on the wall, and on the other side, the closest pillar is spaced 7 µm from the wall as can be seen in the Figure 11B.

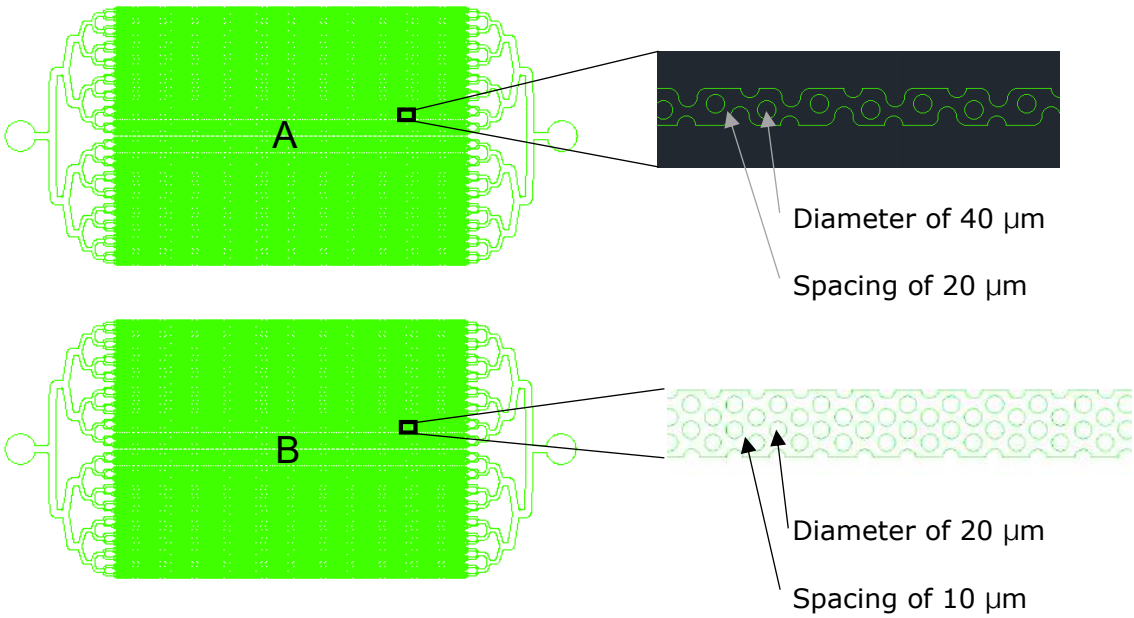

Figure 11 - (A) Representation of device A, its channel constitution and pillar characteristics (B) Representation of device B, its channel costitusion and pillar characteristics.

The device C has a length of 5,39 cm and a width of 1,76 cm, it is constituted of six separated channels with a length of 4 cm and a width of 2,5 mm, the channels are filled with small pillars with a diameter of 40 µm and a spacing of 20 µm, the pillars close to the wall are spaced from it by 35 µm and 63 µm, to prevent problems that may occur with the bounding process, on that sense, by the outlet side the ends of the channels don't have pillars to prevent DNA to get stuck and facilitate the flow (Figure 12).

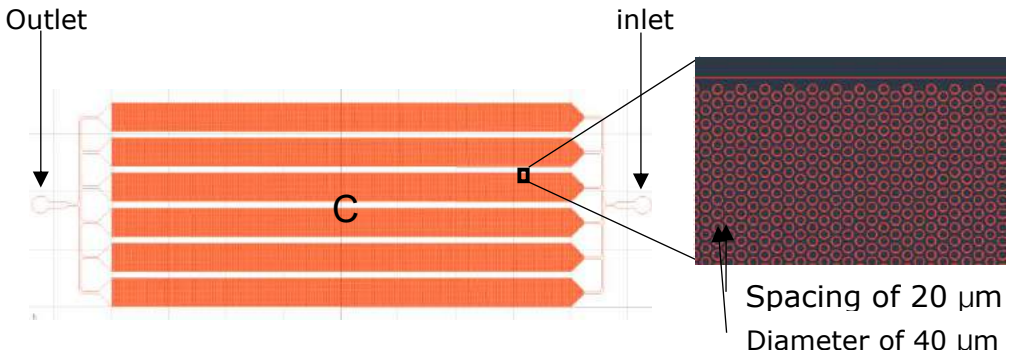

Figure 12 - Representation of device C, its channel constitution and pillar characteristics.

After drawing the designs, two different heights (20 µm and 50 µm) were chosen to be tested further in the project. The height was chosen having the diameters of the pillars in mind, preventing problems with the later process of bounding. The inlet and outlet have a diameter of 1,5 mm in all the different devices.

3.1.2. – Fabrication of a silicon master

Photolithography is the collective name for a group of techniques that uses a beam of photons to transfer a pattern on a thin film of suitable materials over to a subtract, such as a silicon wafer[84,85] The process involved in this method involves a large number of steps that are executed inside a clean room. Fabrication of the silicon master mold is performed using a SiO2 hard mask for the silicon dry etching process. For this purpose, a 1 um thick plasma enhanced chemical vapor deposition (PECVD) SiO2 layer is firstly deposited on a single-side polished (1 0 0) 200mm Si wafer using a CVD system (MPX from SPTS). The wafer was exposed to hexamethyldisilazane (HDMS, Sigma Aldrich, USA) vapor prime to improve the adhesion of the photoresist to the sample, obtained by spin coating of 1,2 µm of AZP4110 (Microchemicals GmbH, Germany) (Figure13A) on an SÜSS MicroTec optical track (SÜSS MicroTec AG, Germany) (figure13B). After thermal treatment, the substrate is introduced in the stepper, an optical projection tool.

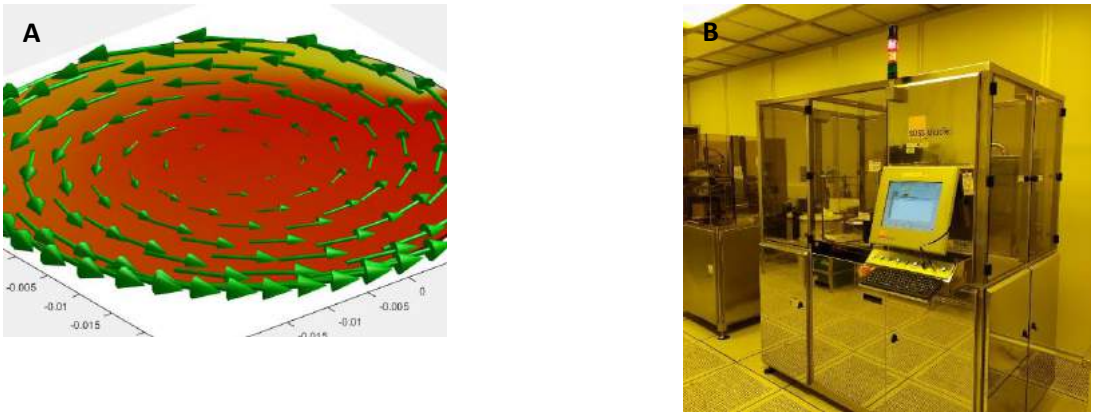

Figure 13 – (A) Representation of the spin coating of 1,2 µm of AZP4110; (B) INL SÜSS MicroTec AG.

In the next step, a Direct write laser (DWL 2000 Heidelberg Instruments) was used on the wafer through a mask and a reduction lens system on a small region of the wafer to promote a high resolution, this process is then repeated to the full area of the wafer by a combination of stepping and scanning operations, to achieve the desired image. During the exposure, there are two different methods, a positive and a negative, if the illuminated region becomes more acidic, the material is called a positive photoresist, while in the opposite case the material is called a negative photoresist and the area becomes less acidic (Figure 14).

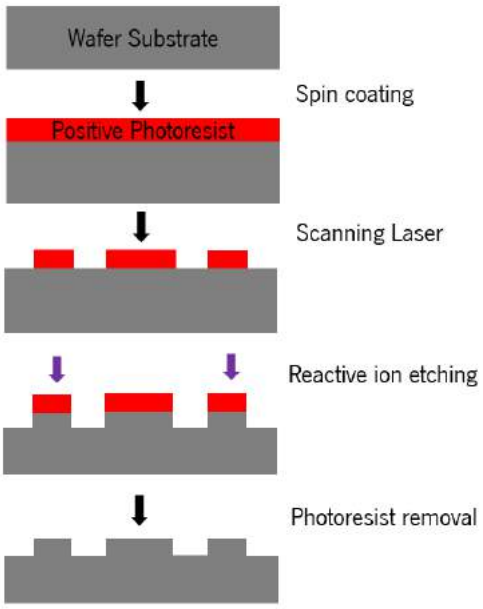

Figure 14 – Direct writing on a wafer using UV light and positive photoresists.

For this project, we used a positive Photoresistm, AZP4110 as mentioned before. Finally, the wafer is baked at a high temperature where the exposed photoresist was developed with AZ400K (Microchemicals GmbH, Germany), and the wafer was rinsed with deionized water and dried. Etching of SiO2 has been completed on a reactive ion etching (RIE) tool (APS from SPTS) with C4F8 etching chemistry followed by removal of the photoresist, striped with an oxygen plasma (PVA GIGAbatch 360 M from Tepla). The silicon wafer was then etched by a dry etching process performed on an inductively coupled plasma (ICP) - RIE tool (Pegasus from SPTS), using an SF6/C4F8 plasma, to transfer the SiO2 mask features to the bulk silicon. The top remaining SiO2 mask was removed on APS from SPTS. Trench depth was measured using a surface profilometer (KLA - Tencor P-16 Surface Profiler) until the desired depth of 20 and 50 μm was reached[86].

3.1.3 - Fabrication of PDMS devices

Soft lithography is the collective name for a group of techniques used for the fabrication of microstructures for biological applications that are based on the printing and molding via elastomeric stamps with patterns of interest[87–89].

The use of soft lithography has several benefits relatively lower cost, easier setup, high throughput, and a nanometer-to-micrometer precision pattern resolution. Despite those benefits, soft lithography needs the utilization of another lithography method such as photolithography or e-beam lithography to fabricate the stamp master[88].

To prepare the mold a solution of PDMS is used in order to create a slide frame for further use. To prepare a solution of PDMS first, the silicon elastomer curing agent (crosslinker) and silicon elastomer base (prepolymer) (SYLGARD™ 184 Silicone Elastomer Kit) were weight with a proportion of 1:10 into a 100 ml cup, the densities of both are similar to 1, so using 60 g of PDMS prepolymer + 6 g of crosslinker will give about 60 ml of PDMS (Figure 15A). Then it was mixed until it bubbles and the mixture becomes cloudy and white. Finally, the solution is put inside the desiccator under vacuum until the solution expands enough to reach the top of the cup due to the bubbles, the process may be repeated until all the bubbles have disappeared. The PDMS can then be used or stored in the freezer at -20°C until it's necessary to use, that way the PDMS will not cure or harden, for future use (Figure 15B).

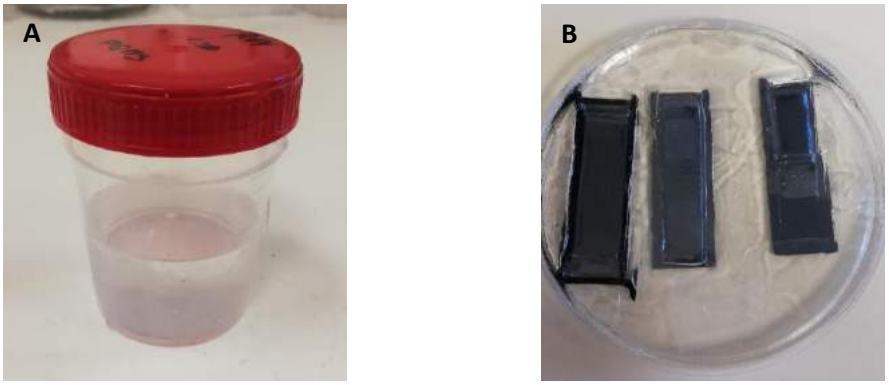

Figure 15 – (A) PDMS container after being removed from the freezer; (B) Petri dish with the devices inside under a layer of PDMS ready to be cut.

To begin the production of the devices, first, the cut wafer is placed inside a petri dish which will be fully covered in PDMS (Figure 15B). After that, the petri is put inside the desiccator under vacuum until, to get any formed bubbles are removed, then it's put inside a stove at 65 °C – 80 °C during the night to cure, and finally, it is removed to cool at room temperature. At this stage, the device can be cut from the frame and then stored (Figure 16A), to repeat the production of new replicas of the device, PDMS is poured over the master wafer already located in the petri dish, the thickness of the layer is around 4 – 5 mm.

After that, it's repeated the process of degassing in the desiccator (Figure 16B), this time the vacuum should be on until the top surface of the PDMS is full of bubbles, the process is repeated and then let to rest for about 10 to 20 mins until the bubbles are not visible. The petri dish is then put into the oven at 65 °C – 80 °C for at least 2h. After the PDMS is fully cured it can be stored at room temperature for long periods. This process can be repeated to create more replicas of the devices. To remove the replica the PDMS was cut around the pattern, then peeled off using tweezers, to protect the face with the imprinted pattern we used clear duck tape so the replica could be stored. Before it gets to the next steps the replica needs to get the inlet and outlet punched using a 1,5mm puncher.

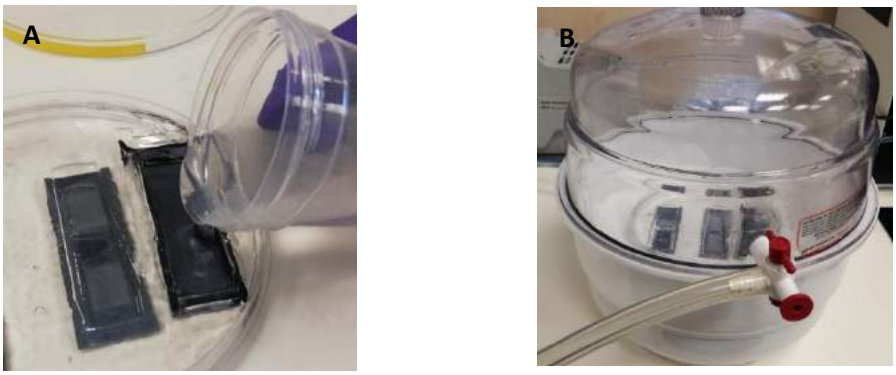

Figure 16 – (A) PDMS being poured on the design; (B) Process of degassing the recently poured PDMS in the desiccator

Before the devices can be used, they need to be bounded with glass slides, in this case, glass slides are used for microscopy since the devices fit them perfectly, for the glass to be prepared for bounding it needs to be cleaned. First, a solution of hellmanex 1% is prepared, Hellmanex® III is an alkaline solution that may be with water to create an effective solution to clean quartz and glass optical components. In this case, the solution was made using a 1% (v/v) of Hellmanex III (10 ml), and 1000 ml of milliQ water.

The cleaning process starts by putting the glass inside the solution of Hellmanex for about 10 minutes to ensure all the surface of the glass slide gets treated. After that time the glass is carefully cleaned using a water gun and further dry using a nitrogen gun, to ensure the glass slide is completely dry and clean it was put in the oven for 2 min. At this point, the glass slides are ready to be used.

To start the bonding process, it's necessary to make sure the PDMS replica is clean and the plasma cleaner may be cleaned with Ethanol (EtOH) (70%) and precision wipes, after that the replicas and the glass slides can be put inside the plasma cleaner with the active side up, with the door closed, the vacuum pump can be started. To ignite the plasma the chamber needs to be at pressures lower than 300 mtorr, at this point the oxygen may be open (oxygen regulator at 10 psi) the pressure elevates close to 1000 mtorr, when the pressure stabilizes at 800 mtorr we can turn the RF power on and the power

level to hight, after some seconds the plasma should ignite with white color, from this point we waited 3 minutes, this extra time ensures that the surface of the PDMS is fully active. Finally, the RF power can be turned off and the oxygen closed, after waiting for the pressure to get lower than 300 mtorr, we can turn off the pump and slowly open the valve until the chamber gets to room pressure. As soon as the PDMS replica and glass slide are removed from the chamber and before bonding them together it's necessary to check for any fiber or impurities, with the glass slide resting on the table slowly join them together applying a small amount of force on top of the PDMS so all the pillars get bonded with the glass.

After the bonding step, the device must be checked under a microscope so that way is possible to identify any problem that occurred during the previous steps, the device must not be stored and should be used right away, which prevents the active surface to be lost. To connect the device to the syringe, an Ethyl-Vynil-Acetate (EVA) tube was used with a 30 cm length and 1,5 mm outer diameter, these tubes were connected to the inlet and the outlet, and on the inlet tube was put a connector fitting to connect the tube to the syringe (Figure 17).

Figure 17 – Plasma Cleaner used to bond the PODMS devices with the Glass slides (Harrick Plasma Inc)

3.2. – Solutions and Reagents

3.2.1 – 0.1% (3-glycidyloxypropyl)trimethoxysilane (GPTMS) (v/v)

GPTMS works as a crosslinker between the PDMS surface and the polymer in use (Chitosan in this particular case). To produce this solution we started by making a 1% stock solution of GPTMS, using 9900 µl of ethanol 100%, adding to this 100 µl of the GPTMS 98% (Sigma-Aldrich). Next using the stock

solution of 1% GPTMS it's possible to make the desirable 0,1%, to make that we use 900 µl of 100% Ethanol plus 1% GPTMS.

1% GPTMS = 9900 µl (100% Ethanol) + 100 µl (98% GPTMS)

0.1% GPTMS = 900 µl (100% Ethanol) + 100 µl (1% GPTMS)

3.2.2 – NaCl 0.15 M

The NaCl 0,15 M is important to clean the device after the previous step, to remove the excess chitosan, and to make the next solutions. To make 100 ml of NaCl 0,15 M we need 0,8766 g of NaCl (Sigma). Then the NaCl powder is dissolved in MilliQ water using a magnet and a hot plate. The solution is finally filtered and stored at room Temperature.

0,15 mol/l * 0,1 l * 58,44 g/mol = 0,8766 g (NaCl)

NaCl 0,15 M = 100 ml (MilliQ water) + 0,8766 g (NaCl)

3.2.3 – 1% Chitosan Oligomer (w/v)

To make the chitosan solution, first, a 1% Acetic acid (v/v) in NaCl 0,15 M solution is prepared, pouring 100 ml of NaCl 0,15 M and then adding 1000 ul of acetic acid (Sigma-Aldrich). Using 100 ml of the 1% Acetic acid (v/v) and adding 1g of chitosan oligomer, after dissolving we obtained the desirable solution of 1% Chitosan Oligomer (w/v) that can be stored at room temperature.

1% Acetic acid = 100 ml (NaCl 0,15 M) + 1000 ul (Acetic Acid)

1% Chitosan Oligomer = 100 ml (1% Acetic acid) + 1g (Chitosan Oligomer)

3.2.4 - 2-(N-morpholino)ethanesulfonic acid (MES) 10 mM (w/v)

MES chemical structure contains a morpholine ring, it has a molecular weight of 195,24 g/mol and the chemical formula is $C_6H_{13}NO_4S$. To make a solution of MES 10 mM we start by filling a 100 ml glass with MilliQ water and then pouring 0,19524 g of MES, after dissolving we obtain the final solution of MES 10 mM (w/v). The solution is then measured and asserted to a pH of 5.

0,01 mol/l * 0,1 l * 195.24 g/mol = 0,1952 g (MES)

MES 10 mM = 100 ml (MilliQ water) + 0,1952 g (MES)

3.2.5 – Tris-Base 50 mM

Tris-base 50 mM at a pH8, Tris-base has a molecular weight of 121,14 g/mol, and the chemical formula is $C_4H_{11}NO_3$. To make that solution we filled a 100 ml glass with MilliQ water and then dissolved 0,6057 g of Tris-Base.

0,05 mol/l * 0,1 l * 121,14 g/mol = 0,6057 g (Tris-Base)

Tris-Base 50 mM = 100 ml (MilliQ water) + 0,6057 g (Tris-Base)

3.2.6 - Low molecular weight salmon sperm DNA

We started by doing a stock solution of 10 mg/ml salmon DNA (SDNA), by dissolving 0,1 g of the DNA powder in 10 ml of tris-base. Then we prepared an intermediate solution of 0,1 mg/ml of the DNA by diluting 10 µl of the stock solution in 999 µl of tris-base. Lastly, we prepared the final solution of 0,001 mg/ml (1 ng/µl) by diluting 10 µl of the intermediate solution in 1 ml of conditioning buffer MES.

10 mg/ml Salmon DNA = 0,1g (DNA) + 10 ml (Tris-Base)

0,1 mg/ml Salmon DNA = 10 µl (10 mg/ml Salmon DNA) + 999 µl (Tris-Base)

1 ng/µl Salmon DNA = 10 µl (0,1 mg/ml Salmon DNA) + 1000 µl (MES)

3.2.7 – Elution Buffer

The elution buffer is composed of Tris-HCl and Ethylenediaminetetraacetic acid (EDTA), the molecular weight of the Tris-HCl is 157,6 g/mol and the weight of the EDTA is 292,2 g/mol. To prepare the solution we start by filling a 100 ml glass with MilliQ water and then dissolving 0,1576 g of Tris-HCl and 0,0292 g of EDTA. The solution must be set to a pH of 10.

0,01 mol/l * 0,1 l * 157,6 g/mol = 0,1576 g (Tris-HCl)

0,001 mol/l * 0,1 l * 292,2 g/mol = 0,0292 g (EDTA)

Elution Buffer = 100 ml (MilliQ water) + 0,1576 g (Tris-HCl) + 0,0292 g (EDTA)

3.3 – Experimental protocol

The experimental procedure was done using 1 ml syringes, a syringe pump, and with the help of a microscope (Nikon eclipse MA200). The device was put on the microscope while the pump and residues reservoir were on either side, all the different experiments have been done using three replicas at the same time (Figure 18).

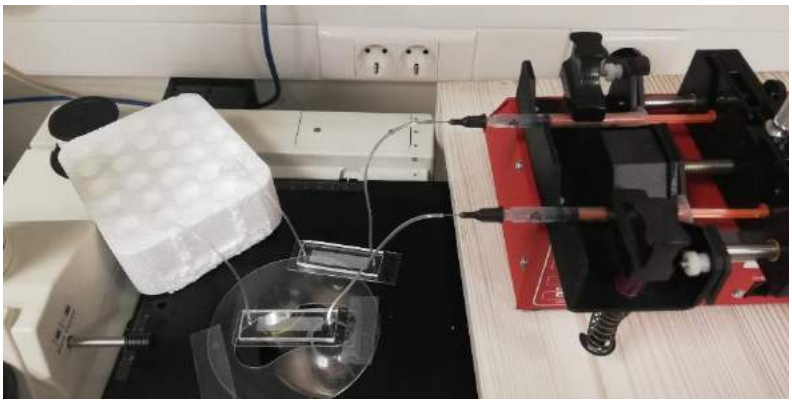

Figure 18 – Work setup for the experimental protocol using the microscope to monitor the experiment.

3.3.1 – Device Functionalization

The first step is responsible for increasing the surface wettability of the device by doing a washing step using 300 µl of 100% Ethanol, this step is done with a flow rate of 20 µl/min. During this project, an alternated-direction flow was tested as well using various flow rates.

Next 600 µl of the solution of GPTMS (0,1% (v/v) in ethanol) is run through the device at the same flow rate as before using only the normal flow rate, this process takes normally at least 30 min.

Then washing the device with 300 µl ethanol 100% at a flow rate of 20 µl/min, which takes normally 15 mins, to remove any excess GPTMS.

After that, the device can finally be functionalized by flowing 300 µl/min of 1% Chitosan oligomer, at a flow rate of 20 µl/min, after the 15 minutes needed to flow the full solution, a period of 1h of incubation is added to promote a better functionalization of the device, different tests were done on this step to get a more optimized functionalization.

To remove excess chitosan we used 900 µl of 0,15 M NaCl at a flow rate of 20 µl/min taking 45 minutes to finish the full process.

3.3.2 – DNA Purification and Concentration

This project used Salmon DNA was the one chosen because of the base pares (bp) number being close to the ctDNA, having close to 300bp.

At this stage of the work, in every step, samples were collected to be quantified later. First is a conditioning step, responsible for decreasing the pH of the device using 200 ul of MES with a pH of 5, at a normal flow rate of 20 µl/min for approximately 10 minutes, this step helps the binding of the DNA. Here we collected one sample of 200 µl (Figure19 C).

Now, for the Binding step using 1000 µl of the DNA solution made before is run through the device at a flow rate of 100 µl/min taking 10 minutes, then a withdraw step at the same flow rate is included to get a better bind of the DNA. After that, the solution is collected over another flow to five Eppendorf containing 200 µl each (Figure19 B1 to B5), the total time to finish this step is around 30 minutes (10+10+10).

To clean the remaining DNA that did not get bound with the chitosan in the walls of the device, a washing step is included, to do that 500 µl of MES (pH 5) was used at 20 µl/min flow rate. Here two samples of 250 µl each were collected (Figure 19 C1 and C2).

Finally, to remove the DNA from the device, 300 µl of the buffer solution produced before was used at a flow rate of 20 µl/min. The buffer has a ph of 10 to promote a drastic difference in the bond between the DNA and the chitosan previously at pH 5. On This final step, the samples collected are smaller having 50 µl for each sample (Figure 19 E1 to E6).

Figure 19 – Sample collection for further quantification on the Qubit.

3.3.3 – DNA Quantification

The DNA was quantified using the Qubit, it was used the 1X dsDNA High Sensitivity (HS) and Broad Range (BR) Assay Kits, and Qubit™ assay tubes (Thermo Fisher Scientific, Aalst, Belgium), these tubes have 500 µl thin-walled polypropylene tubes, the standards that come with the kit have 0 and 10000 ng/ml. To prepare the standard solutions 10 µl of the standard was added to 190 µl of 1X dsDNA HS working solution and then measured on the Qubit to get the calibration line (Figure 20). To prepare the solution we want to measure, from a range of 1 – 20 µl, 20 µl was used of the solution added to 180 µl of working solution and then measured by the Qubit.

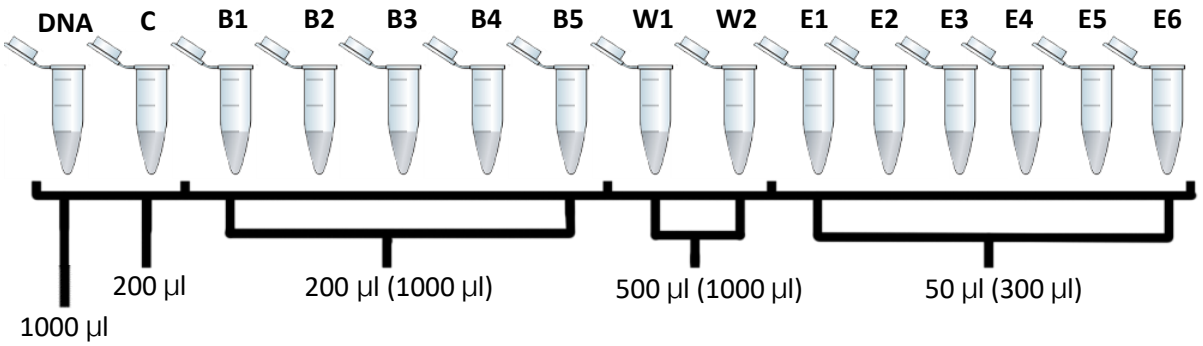

Figure 20 – Collection of the different samples for further quantification on the Qubit and concentrations.

4 - Results and Discussion

4.1 – Selection of best geometry

The device height was the first important variable, being the 20 µm height devices the first to be compared using the standard protocol. Device A had a good recovery compared to the amount of DNA bounded having an elution of 49,48%. This device had some problems during the second step of the Binding, the withdraw, creating some bubbles, this had to do with the pressure created inside the device. This problem resulted in the binding having only 77,06%. This device had a slightly high standard deviation of 6,92% on the binding and 8,80% on the Elution, having some devices with great elutions and others with bad elutions, not giving consistent results (Figure 21) (Table 2).

Table 1 – Binding, recovery, and elution of the device A with 20 µm height using the normal protocol.

	BINDING	ELUTION	RECOVERY
D1	82%	61%	50%
D2	82%	48%	39%
D3	67%	39%	27%
Mean	**77,06%**	**49,48%**	**38,62%**
Standard Deviation	6,92%	8,80%	9,52%

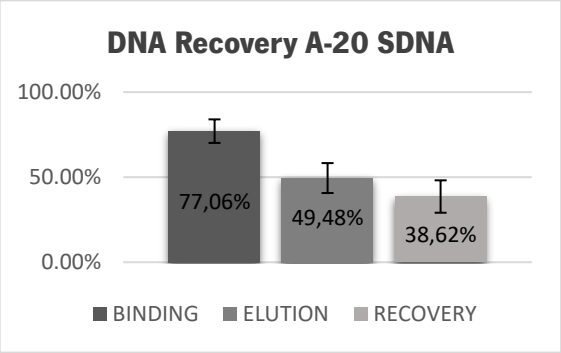

Figure 21 – Binding, recovery, and elution of the device A with 20 µm height using the normal protocol.

During the experiment, there were some losses in the binding and washing steps, losing 22,94% of the initial DNA. In the end, 38,44% of the DNA stayed inside the devices (Figure 22), this relatively low number may be due to the high losses on the other steps and the relatively good recovery rates.

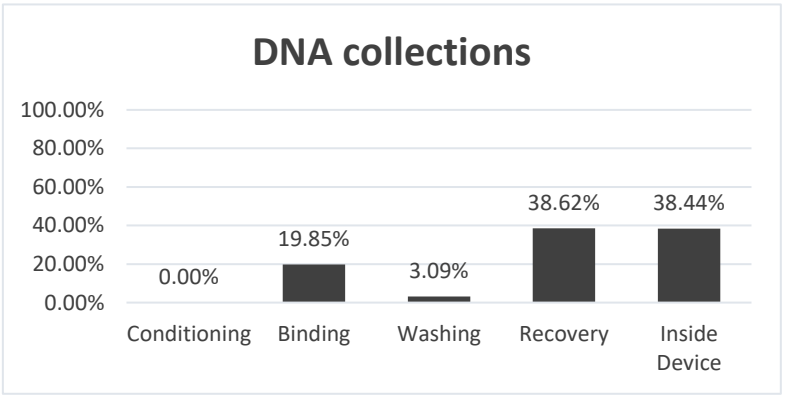

Figure 22 – Representation of the DNA losses and recovery throughout the experiment for device A with 20 µm height.

The device B was then tested, having the same problems as the previous devices, forming bubbles on the withdraw step of the binding. This time the recovery rates were close to the other device, 37,12% however, the binding step was better, 87,16%, resulting in a lower elution of 42,58%. The standard deviation is also lower, 2,24% for the binding and 1,1% for the elution, despite that, during the experiment, because of the high pressures created inside the devices, one of them leaked throw the inlet during the first phase of the binding step, and was not possible to recuperate, reducing the number of samples to two (Figure 23) (Table 3).

Table 3 – Binding, recovery, and elution of the device B with 20 µm height using the normal protocol.

	BINDING	ELUTION	RECOVERY
D1	86%	42%	36%
D2	89%	43%	39%
Mean	**87,16%**	**42,58%**	**37,12%**
Standard Deviation	2,24%	1,20%	1,99%

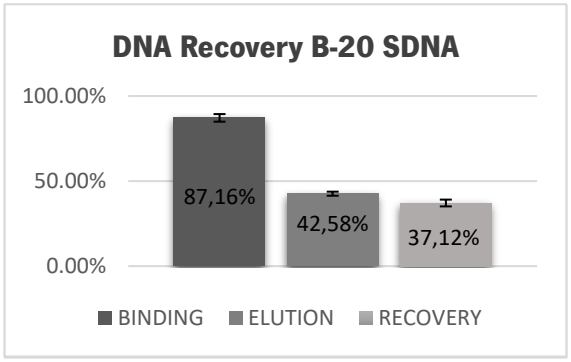

Figure 23 – Binding, recovery, and elution of the device B with 20 µm height using the normal protocol.

The amount of DNA lost on these devices was a little less than the previous ones, being all in the binding step with only 12,84% of all DNA. However, this time the quantity of DNA lost to the device is higher with 50,03% of the DNA getting stuck inside the device (Figure 24), this may be due to the number of pillars in the small channels not letting the DNA flow as easily as in the other device.

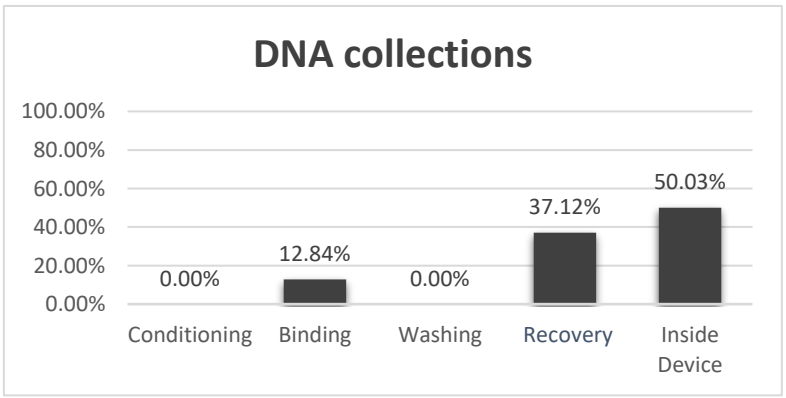

Figure 24 – Representation of the DNA losses and recovery throughout the experiment for device B with 20 µm height.

Device C had again the same problems that the other had with the withdraw of the binding step. On the other hand, the recovery rates were better at 42,02%, and the binding step was almost perfect at

98,71%, consecutively the elution step was a little less compared to the others with 42,62%, but having the amount of DNA bonded, the overall performance of this device is better than the previous ones. The only problem found was the standard deviation which is still a bit high on the recovery and elution, with 6,89% and 7,35% respectively. The standard deviation for the binding is good with only 1,03% (Figure 25) (Table 4).

Table 4 – Binding, recovery, and elution of the device C with 20 µm height using the normal protocol.

	BINDING	ELUTION	RECOVERY
D1	99%	36%	35%
D2	100%	39%	39%
D3	97%	53%	51%
Mean	**98,71%**	**42,62%**	**42,02%**
Standard Deviation	1,03%	7,35%	6,89%

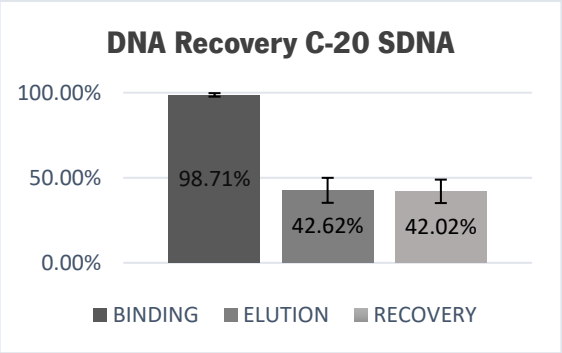

Figure 25 – Binding, recovery, and elution of the device C with 20 µm height using the normal protocol.

The amount of DNA lost on these devices was almost none, 0,44% on the binding step and 0,84% on the washing step. However, this time the quantity of DNA still inside the device at the end of the experiment was a little bit higher at 56,69% (Figure 26), this could be because of the height of the device since this time the channels are a lot bigger and this device as a feature to help the flow of the DNA.

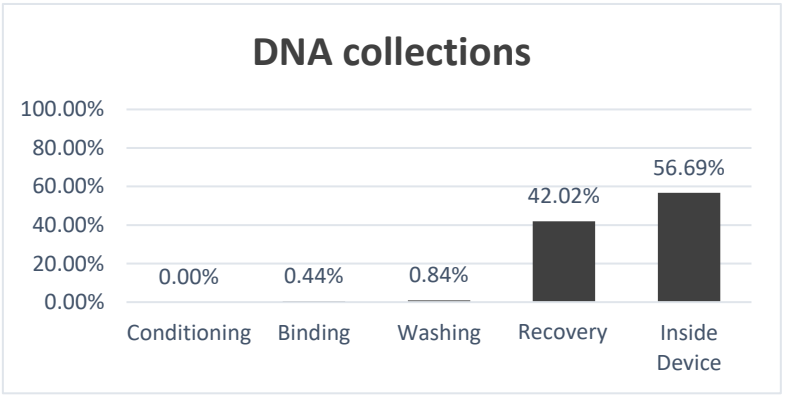

Figure 26 – Representation of the DNA losses and recovery throughout the experiment for device C with 20 µm height.

Comparing the three devices with 20 µm height, device C stands out from the others, having an overall better performance, with good binding and recovery, but still having some problems that were expected to be resolved by changing the height of the device.

Then the same devices were tested with the 50 µm height, starting with device A, this time there were no problems with the withdraw of the binding step, not forming bubbles. This time the binding is still not perfect with 81,58% but better than the 20 µm device, having a better recovery and elution, 42,12% and 51,89% respectively. The results have slightly better consistency having a standard deviation of 9,08% for the binding step, 4,79% for the recovery step, and 4,82% for the elution step (Figure 27) (Table 5).

Table 5 – Binding, recovery, and elution of the device A with 50 µm height using the normal protocol.

	BINDING	ELUTION	RECOVERY
D1	87%	45%	39%
D2	89%	55%	49%
D3	69%	56%	38%
Mean	**81,58%**	**51,89%**	**42,12%**
Standard Deviation	9,08%	4,82%	4,79%

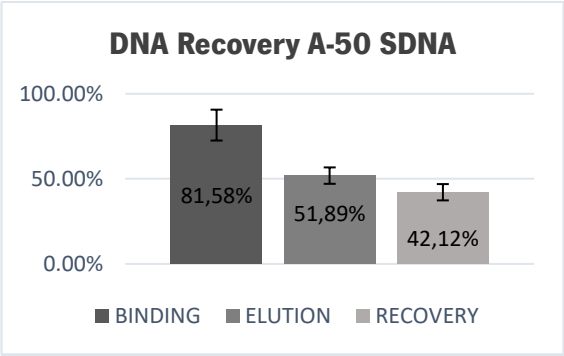

Figure 27 – Binding, recovery, and elution of the device A with 50 µm height using the normal protocol.

As said before, the binding step was better so the DNA lost was less as well, with a total loss of 18,42%. The good recovery and low loss of DNA helped to have a low quantity of DNA stuck on the device, with 39,46% (Figure 28). The overall better results on these devices show that the 50 µm height is slightly better and has fewer problems with the practical steps.

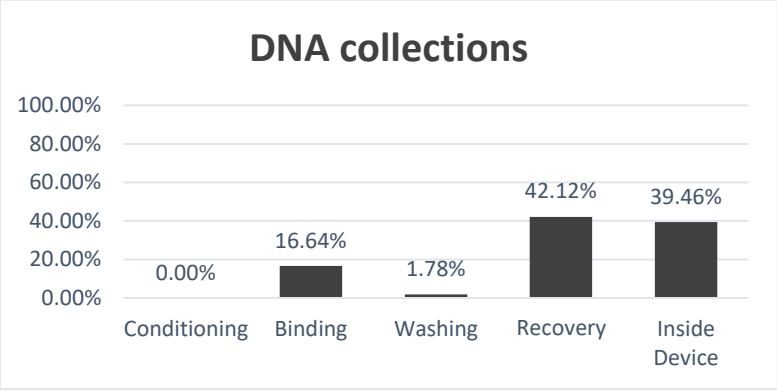

Figure 28 – Representation of the DNA losses and recovery throughout the experiment for device A with 50 µm height.

Device B this time had slightly better recovery rates of 38,22%, compared with the 20 µm devices. The binding is a little bit less with 84,52%. Finally, the elution was better at 44,86%. The results of the recovery and elution are inconsistent with standard deviations of 13,09% and 13,48% (Figure 29) (Table 6).

Table 6 – Binding, recovery, and elution of the device B with 50 µm height using the normal protocol.

	BINDING	ELUTION	RECOVERY
D1	81%	35%	28%
D2	84%	40%	34%
D3	88%	60%	53%
Mean	**84,52%**	**44,86%**	**38,22%**
Standard Deviation	3,47%	13,48%	13,09%

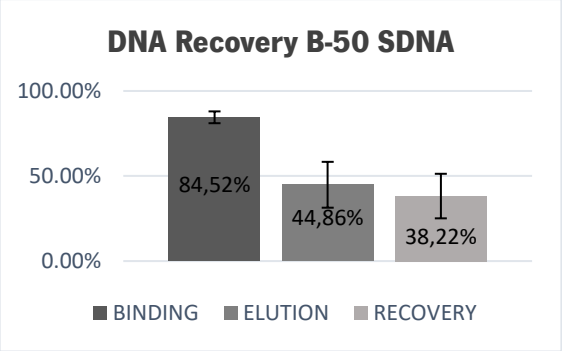

Figure 29 – Binding, recovery, and elution of the device B with 50 µm height using the normal protocol.

The losses were higher than the 20 µm device reaching 15,48% of all DNA. The amount of DNA retained on the Device was 46,30% of all DNA which is still a very high number (Figure 30).

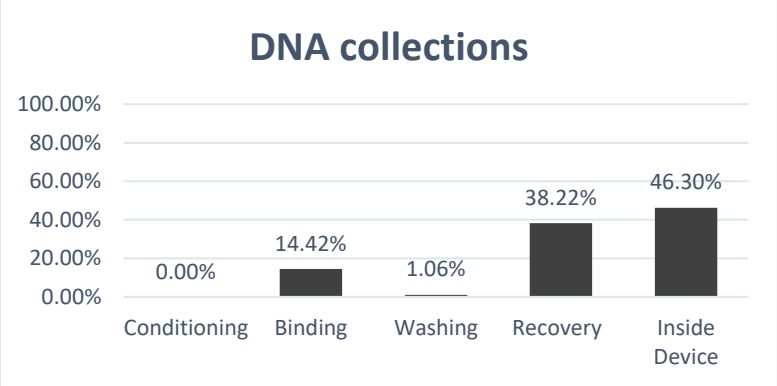

Figure 30 – Representation of the DNA losses and recovery throughout the experiment for device B with 50 µm height.

Device C has the best binding, 93,26%, of the 50 µm devices, being slightly lower than the 20 µm device C, but at this range, nothing that relevant. The recovery rates and elution were good having 47,25% and 50,77% respectively. The results between the triplicates are closely the same as the ones for

the device C 20 µm height, being slightly high at 5,85% for the binding step, 8,13% for the recovery, and 6,07% for the elution (Figure 31) (Table 7).

Table 7 – Binding, recovery, and elution of the device C with 50 µm height using the normal protocol.

	BINDING	ELUTION	RECOVERY
D1	97%	58%	57%
D2	85%	51%	43%
D3	98%	43%	42%
Mean	**93,26%**	**50,77%**	**47,35%**
Standard Deviation	5,85%	6,07%	8,13%

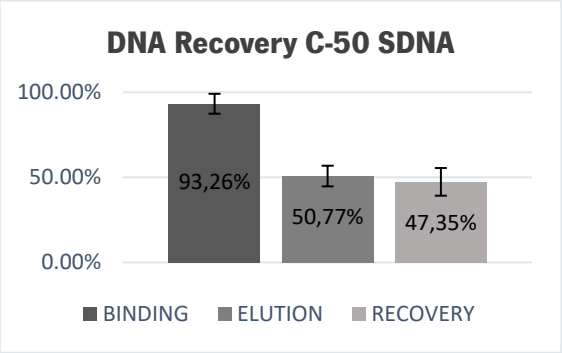

Figure 31 – Binding, recovery, and elution of the device C with 50 µm height using the normal protocol.

This device had very good binding, not losing much DNA, resulting in only 6,74% of all DNA lost. The DNA left in the device was 45,91%, which compared to the others is a good result, being much better than its counterpart (Figure 32). The overall results of these devices were better than all the previous ones.

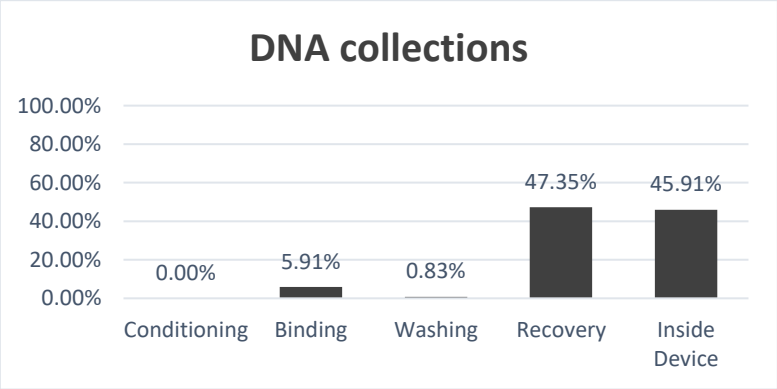

Figure 32 – Representation of the DNA losses and recovery throughout the experiment for device C with 50 µm height.

By analyzing the results, the best-performing device was device C with 50 µm height, having the best binding and recovery of all. The small difference between the binding from the Device C 20 µm and Device C 50 µm is not of preoccupancy since it is above the 90% mark, this is probably due to the greater area for the DNA to flow without contacting the walls or pillars, however, the difference of almost 8% in the recovery and elution and 5% on the recovery are more significant (Figure 33B), this has probably the same cause being easily to extract the DNA.

Device A is not as good as Device C but having the best elution made him interested to progress for the next phase of tests (Figure 33C), where the binding step will be focused to try and get a better binding for this device since it is his problem.

Device B had a similar but worst performance compared to the others, having a little better binding than Device A, but falling behind on all the other parameters (Figure 33A), and being dropped from the project.

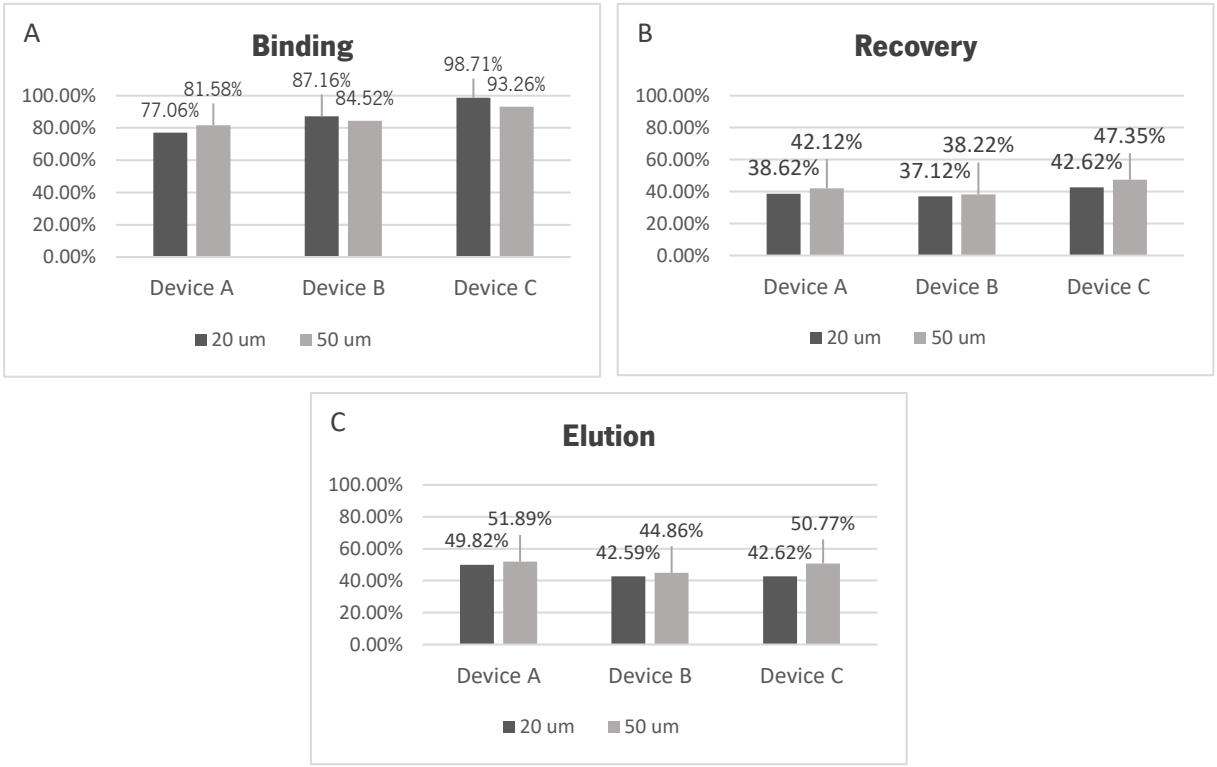

Figure 33 – (A) Comparation between the three devices for the binding step; (B) Comparation between the three devices for the recovery; (C) Comparation between the three devices for the elution.

4.2 – Optimisation of the protocol

4.2.1 – Optimise timing

Before starting the optimization processes some tests were performed on the normal protocol but now increasing the flow rate speed of the washing step between the binding and the elution step, being increased from 20 µl/min to 100 µl/min, to reduce in 20 min the time of the experiment, without having changes on the results. The first, device A with 50 µm height, this time had better bindings of 88,21% and a similar recovery of 41,64% which means that the elution was slightly lower at 47,20%, but overall constant and similar results as expected (Figure 34) (Table 8), and not losing that much DNA, 11,79% (Figure 35), remaining the main focus trying to get a better binding while not losing on the recovery or elution. On this device, the change of speed on the last washing speed did not have any influence on his performance.

Table 8 – Binding, recovery, and elution of the device A with 50 µm height using a higher washing flow rate.

	BINDING	ELUTION	RECOVERY
D1	88%	48%	42%
D2	88%	46%	41%
Mean	**88,21%**	**47,20%**	**41,64%**
Standard Deviation	0,15%	0,86%	0,98%

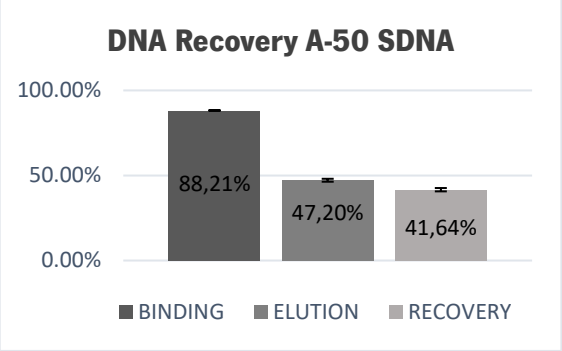

Figure 34 – Binding, recovery, and elution of the device A with 50 µm height using a higher washing flow rate.

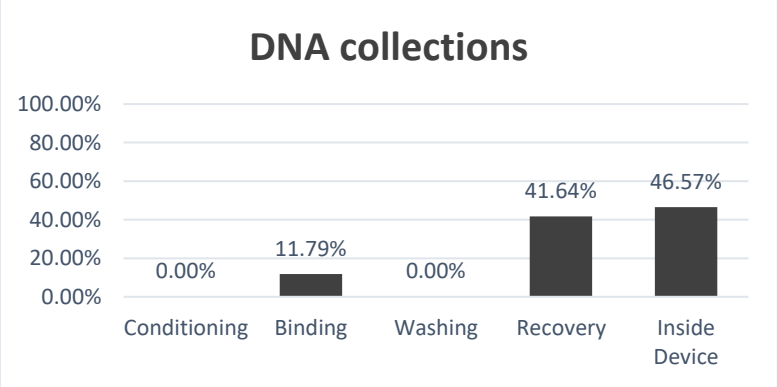

Figure 35 – Representation of the DNA losses and recovery throughout the experiment for device A with 50 µm height using a higher washing flow rate.

Device C had mostly the same results as before, not changing much, but still with a substantial standard deviation of 8,866% for the recovery (Figure 36) (Table 9). The DNA loss was practically the same, 4,53% (Figure 37), but it didn't have a direct impact on the overall performance of the device. The main focus of this device was to try and increase the recovery rate, while not decreasing the binding. For this device, the changes didn't affect the results, demonstrating that they can be done and are a great way to reduce the time of the protocol without having an impact on the results.

Table 9 – Binding, recovery, and elution of the device C with 50 µm height using a higher washing flow rate.

	BINDING	ELUTION	RECOVERY
D1	100%	58%	58%
D2	97%	52%	50%
D3	90%	45%	40%
Mean	**95,47%**	**51,63%**	**49,52%**
Standard Deviation	4,24%	5,36%	8,87%

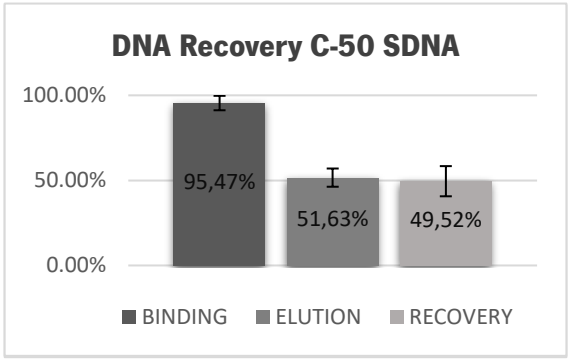

Figure 36 – Binding, recovery, and elution of the device C with 50 µm height using a higher washing flow rate.

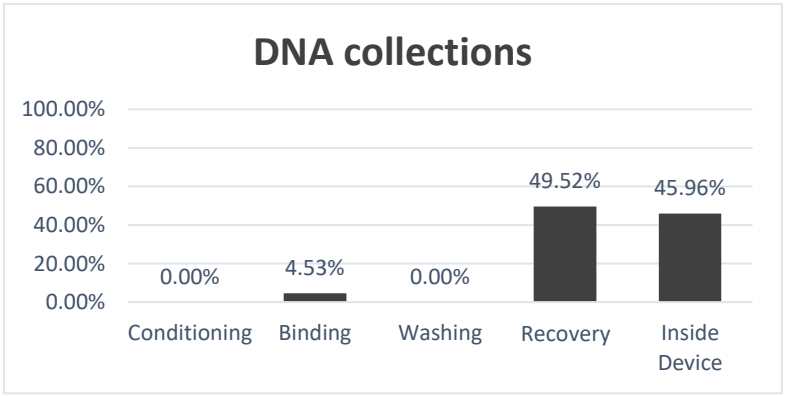

Figure 37 – Representation of the DNA losses and recovery throughout the experiment for device C with 50 µm height using a higher washing flow rate.

4.2.2 – Optimise binding

After getting the confirmation related to the performance of the devices, the main focus was to improve them and to try and modify the protocol so it is more efficient and even faster to perform. At this point in the project making a full experiment was taking 4 hours and 50 minutes plus the time to quantify the DNA, taking normally a full day to perform, so one goal was to decrease this time without affecting the efficacy of the protocol.

Before trying to speed up the protocol, reducing the speed was one of the options to try and get a better binding on device A. The binding flow rate speed was reduced to three-quarters of the original speed, 75 µl/min. The results were very consistent but for the second time, one of the devices had leaked and was irrecuperable. Other than that, the results did not change according to what was expected, only having 80,68% of DNA bounded, 38,16% for the recovery, and 47,34% for the elution (Figure 38) (Table 10). The DNA lost was on the high end of the acceptable range, 19,32%, but it's not significant for the test.

Table 10 – Binding, recovery, and elution of the device A with 50 µm height using 75 µl/min binding flow rate.

	BINDING	ELUTION	RECOVERY
D1	83%	46%	38%
D2	78%	49%	38%
Mean	**80,68%**	**47,34%**	**38,16%**
Standard Deviation	2,42%	1,43%	0,01%

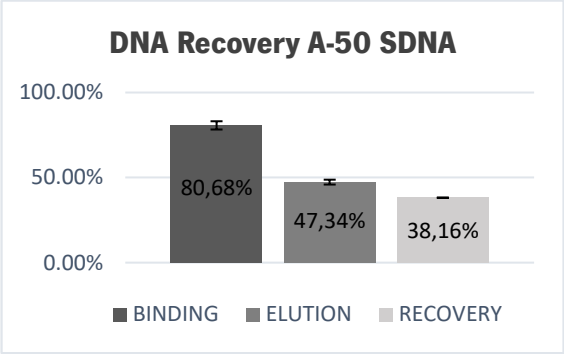

Figure 38 – Binding, recovery, and elution of the device A with 50 µm height using 75 µl/min binding flow rate.

4.2.3 – Optimise elution

Next, to improve the recovery on device C, and increase the speed as well, the flow rate of the elution step was increased to three times the normal flow rate, 60 µl/min. Again, the results were not desirable, even getting worst results on the binding step of 88,55% which are not related to the current experiment. The recovery and elution were similar to the normal protocol (Figure 39) (table11).

Table 11 – Binding, recovery, and elution of the device C with 50 µm height using 60 µl/min elution flow rate.

	BINDING	ELUTION	RECOVERY
D1	94%	54%	51%
D2	88%	51%	45%
D3	83%	49%	40%
Mean	**88,55%**	**51,36%**	**45,59%**
Standard Deviation	4,72%	2,32%	5,49%

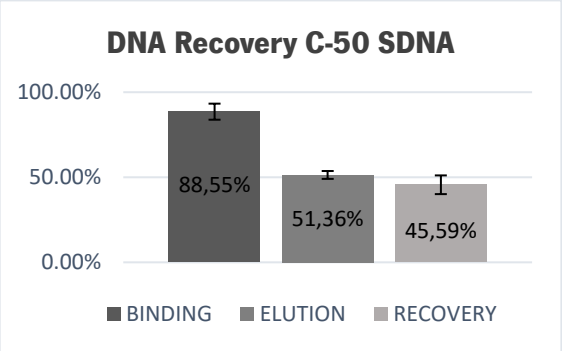

Figure 39 – Binding, recovery, and elution of the device C with 50 µm height using 60 µl/min elution flow rate.

As the previous results were not satisfying, and since this is the best device, another try was done this time using a flow rate of 100 µl/min, so the change was more drastic, and possibly the results could be a bit more revealing and positive towards what's expected. But again, the results were not the expected, with even worst results than the previous try. Now the binding was slightly the same at 89,85%, the recovery way worst at only 34,15%, and the elution at 37,96% (Figure 40) (table 12).

Table 12 – Binding, recovery, and elution of the device C with 50 µm height using 100 µl/min elution flow rate.

	BINDING	ELUTION	RECOVERY
D1	90%	42%	38%
D2	86%	35%	30%
D3	94%	37%	35%
Mean	**89,85%**	**37,96%**	**34,15%**
Standard Deviation	3,28%	2,81%	3,92%

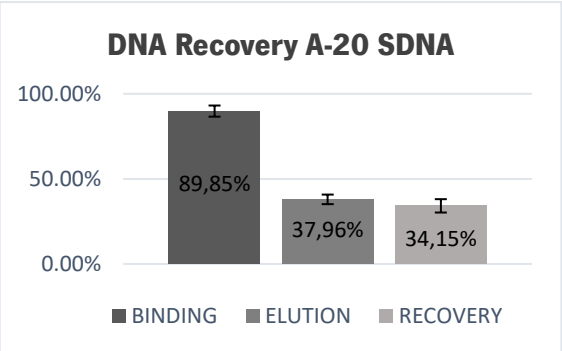

Figure 40 – Binding, recovery, and elution of the device C with 50 µm height using 100 µl/min elution flow rate.

After the previous tests fail a different approach was taken by elevating the pH of the elution buffer to 11, expecting it to provide a stronger interaction with the chitosan, promoting the liberation of the DNA. Device A was the first one to be tested and the results were again not as expected, the binding was better at 89,75% getting close to device C, but these results don't represent the changes done. The recovery and elution, the ones that should have demonstrated the most changes didn't have the results expected being mostly the same as before (Figure 41) (table 13).

Table 13 – Binding, recovery, and elution of the device A with 50 µm height using elution buffer with pH 11.

	BINDING	ELUTION	RECOVERY
D1	91%	50%	46%
D2	93%	44%	41%
D3	86%	55%	47%
Mean	**89,75%**	**49,87%**	**44,64%**
Standard Deviation	2,86%	4,30%	3,09%

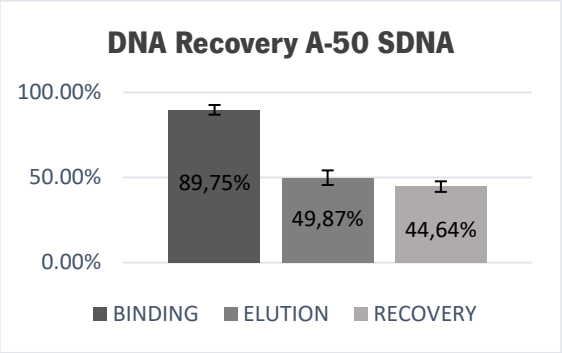

Figure 41 – Binding, recovery, and elution of the device A with 50 µm height using elution buffer with pH 11.

Device C was then tested and the results were again not as expected, the binding was similar to the other that was expected, but the recovery and elution didn't have the results expected even worst than before (Figure 42) (table 14).

Table 14 – Binding, recovery, and elution of the device C with 50 µm height using elution buffer with pH 11.

	BINDING	ELUTION	RECOVERY
D1	97%	36%	35%
D2	96%	53%	51%
D3	97%	47%	45%
Mean	**96,70%**	**45,36%**	**43,84%**
Standard Deviation	0,34%	7,02%	8,14%

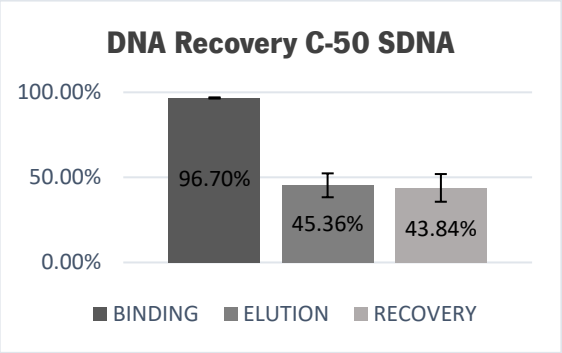

Figure 42 –Binding, recovery, and elution of the device C with 50 µm height using elution buffer with pH 11.

After all the tests and different assessments, the normal protocol with only the alteration of the flow rate speed of the last washing step was the one with the best performance on device C. Device A had good results and at first glance good consistency but from one experiment to another the results changed where it was not expected. The results were not good enough to make up for the sudden changes in the binding step. On this device, the flow rates of the protocol are not so easy to increase to make the process faster, as the device is smaller and the pressures inside rise way faster. There were some fiscal problems with the devices at the inlets and outlets which provoked some losses during the laboratory procedure. The fact that the channels are smaller the bonding step is also harder to get right compared with device C. For all those reasons the device chosen to get used in future experiments and assessments was device C.

4.3 – Proof of concept

For the next steps, the device was to be tested using synthetic plasma spiked with the salmon DNA, in order to be able to test the permeance of the device on a more complex solution. These experiments involve the normal protocol maybe with the alterations that were positive and using the device C as it's the one with the best results. In further testing, device A could be used depending on the device C results. There may be needed changes in the flow rate of the devices since the plasma is a thicker solution and may create higher pressures inside the device.

After the device and protocol have a good performance on the synthetic plasma, the device will be tested using the patient's plasma for further improvements and optimization. Having a final performance assessment for the device and protocol created on this project.

5 - Conclusion

The objective of this project was to develop an inexpensive, single-use microfluidic device to isolate ctDNA from patients with breast cancer in order to compete and surpass the existing methods of ctDNA isolation. This will permit the ctDNA to be analyzed by liquid biopsy and obtain a real-time analysis of the different mutations and the development of cancer allowing for more precise and personalized treatments.

In the end, the best device was able to perform the capture of the DNA and had a good recovery rate of 49,52 % compared with the existing methods that have around 50 % as said in the beginning, being way less expensive alongside other benefices. The devices designed had good behavior when used under the protocol used with the devices with 50 µm height having a better performance. Among them, the best overall device was device C, despite device A having a good performance, close to device C, at the time of this project was not possible to stress test the device having to choose device C as the best for the time being. The trials to optimize the performance of the devices by modifying the protocol did not have the results expected, and no substantial improvement was achieved, but the device can already be compared with commercial kits.

With more time, the device's performance could be further improved, either by exploring other variables or by changing the design of the device altogether.

The future plans for this project are the tests of devices using plasma spiked with DNA, and then after optimizing the protocol for the use of a denser solution, start the tests on plasma from cancer patients, and further optimization.

6 - Bibliography

1. Xu, S. *et al.* The Global, Regional, and National Burden and Trends of Breast Cancer From 1990 to 2019: Results From the Global Burden of Disease Study 2019. *Front Oncol* **11**, (2021).

2. Fisher, R., Pusztai, L. & Swanton, C. Cancer heterogeneity: Implications for targeted therapeutics. *British Journal of Cancer* vol. 108 Preprint at https://doi.org/10.1038/bjc.2012.581 (2013).

3. Heath, J. R. & Davis, M. E. Nanotechnology and cancer. *Annual Review of Medicine* vol. 59 251–265 Preprint at https://doi.org/10.1146/annurev.med.59.061506.185523 (2008).

4. Perakis, S. & Speicher, M. R. Emerging concepts in liquid biopsies. *BMC Medicine* vol. 15 Preprint at https://doi.org/10.1186/s12916-017-0840-6 (2017).

5. Alix-Panabières, C. & Pantel, K. Clinical applications of circulating tumor cells and circulating tumor DNA as liquid biopsy. *Cancer Discovery* vol. 6 Preprint at https://doi.org/10.1158/2159-8290.CD-15-1483 (2016).

6. Yi, X. *et al.* The feasibility of using mutation detection in ctDNA to assess tumor dynamics. *International Journal of Cancer* vol. 140 2642–2647 Preprint at https://doi.org/10.1002/ijc.30620 (2017).

7. Abbosh, C., Birkbak, N. J. & Swanton, C. Early stage NSCLC — challenges to implementing ctDNA-based screening and MRD detection. *Nature Reviews Clinical Oncology* vol. 15 Preprint at https://doi.org/10.1038/s41571-018-0058-3 (2018).

8. Schwarzenbach, H. & Pantel, K. Circulating DNA as biomarker in breast cancer. *Breast Cancer Research* vol. 17 Preprint at https://doi.org/10.1186/s13058-015-0645-5 (2015).

9. de Mattos-Arruda, L. & Caldas, C. Cell-free circulating tumour DNA as a liquid biopsy in breast cancer. *Molecular Oncology* vol. 10 Preprint at https://doi.org/10.1016/j.molonc.2015.12.001 (2016).

10. Chang, Y. *et al.* Review of the clinical applications and technological advances of circulating tumor DNA in cancer monitoring. *Therapeutics and Clinical Risk Management* vol. 13 1363–1374 Preprint at https://doi.org/10.2147/TCRM.S141991 (2017).

11. Yeo, L. Y., Chang, H. C., Chan, P. P. Y. & Friend, J. R. Microfluidic devices for bioapplications. *Small* vol. 7 Preprint at https://doi.org/10.1002/smll.201000946 (2011).

12. Sung, H. *et al.* Global Cancer Statistics 2020: GLOBOCAN Estimates of Incidence and Mortality Worldwide for 36 Cancers in 185 Countries. *CA Cancer J Clin* **71**, 209–249 (2021).

13. Akram, M., Iqbal, M., Daniyal, M. & Khan, A. U. Awareness and current knowledge of breast cancer. *Biological Research* vol. 50 Preprint at https://doi.org/10.1186/s40659-017-0140-9 (2017).

14. Coleman, M. P. *et al.* Cancer survival in five continents: a worldwide population-based study (CONCORD). *Lancet Oncol* **9**, (2008).

15. Beaulac, S. M., McNair, L. A., Scott, T. E., LaMorte, W. W. & Kavanah, M. T. Lymphedema and quality of life in survivors of early-stage breast cancer. *Archives of Surgery* **137**, (2002).

16. Li, C. I., Malone, K. E. & Daling, J. R. Differences in breast cancer stage, treatment, and survival by race and ethnicity. *Arch Intern Med* **163**, (2003).

17. van Uden, D. J. P. *et al.* Metastatic behavior and overall survival according to breast cancer subtypes in stage IV inflammatory breast cancer. *Breast Cancer Research* **21**, (2019).

18. Vranso West, A.-K. *et al.* Division Induced Dynamics in Non-Invasive and Invasive Breast Cancer. *Biophys J* **112**, (2017).

19. Nakhlis, F. & Morrow, M. Ductal carcinoma in situ. *Surgical Clinics of North America* **83**, 821–839 (2003).

20. Iatrakis, G. & Zervoudis, S. Epidemiology of Ductal Carcinoma In Situ. *Chirurgia (Romania)* vol. 116 Preprint at https://doi.org/10.21614/CHIRURGIA.116.5.SUPPL.S15 (2021).

21. Kerlikowske, K. Epidemiology of ductal carcinoma in situ. *J Natl Cancer Inst Monogr* 139–141 (2010) doi:10.1093/jncimonographs/lgq027.

22. Mendonsa, A. M., Na, T. Y. & Gumbiner, B. M. E-cadherin in contact inhibition and cancer. *Oncogene* vol. 37 Preprint at https://doi.org/10.1038/s41388-018-0304-2 (2018).

23. Logan, G. J. *et al.* Molecular drivers of lobular carcinoma in situ. *Breast Cancer Research* **17**, (2015).

24. Feng, Y. *et al.* Breast cancer development and progression: Risk factors, cancer stem cells, signaling pathways, genomics, and molecular pathogenesis. *Genes and Diseases* vol. 5 Preprint at https://doi.org/10.1016/j.gendis.2018.05.001 (2018).

25. Lobbezoo, D. J. A. *et al.* Prognosis of metastatic breast cancer: Are there differences between patients with de novo and recurrent metastatic breast cancer? *Br J Cancer* **112**, (2015).

26. Veronesi, U., Boyle, P., Goldhirsch, A., Orecchia, R. & Viale, G. Breast cancer. *The Lancet* **365**, 1727–1741 (2005).

27. Cronin, K. A. *et al.* Annual Report to the Nation on the Status of Cancer, part I: National cancer statistics. *Cancer* **124**, (2018).

28. Prat, A. *et al.* Clinical implications of the intrinsic molecular subtypes of breast cancer. *The Breast* **24**, S26–S35 (2015).

29. Prat, A. & Perou, C. M. Deconstructing the molecular portraits of breast cancer. *Molecular Oncology* vol. 5 5–23 Preprint at https://doi.org/10.1016/j.molonc.2010.11.003 (2011).

30. Li, Z. H., Hu, P. H., Tu, J. H. & Yu, N. S. Luminal B breast cancer: Patterns of recurrence and clinical outcome. *Oncotarget* **7**, (2016).

31. Hashmi, A. A. *et al.* Prognostic parameters of luminal A and luminal B intrinsic breast cancer subtypes of Pakistani patients. *World J Surg Oncol* **16**, (2018).

32. Mitri, Z., Constantine, T. & O'Regan, R. The HER2 Receptor in Breast Cancer: Pathophysiology, Clinical Use, and New Advances in Therapy. *Chemother Res Pract* **2012**, (2012).

33. Prat, A. *et al.* HER2-Enriched Subtype and ERBB2 Expression in HER2-Positive Breast Cancer Treated with Dual HER2 Blockade. *J Natl Cancer Inst* **112**, (2020).

34. Yin, L., Duan, J. J., Bian, X. W. & Yu, S. C. Triple-negative breast cancer molecular subtyping and treatment progress. *Breast Cancer Research* vol. 22 Preprint at https://doi.org/10.1186/s13058-020-01296-5 (2020).

35. Gluz, O. *et al.* Triple-negative breast cancer - Current status and future directions. *Annals of Oncology* vol. 20 Preprint at https://doi.org/10.1093/annonc/mdp492 (2009).

36. Peng, J., Sengupta, S. & Jordan, V. C. Potential of Selective Estrogen Receptor Modulators as Treatments and Preventives of Breast Cancer. *Anticancer Agents Med Chem* **9**, (2012).

37. Reeder, J. G. & Vogel, V. G. *0. BREAST CANCER PREVENTION*.

38. Zhang, G., Zeng, X. & Li, P. Nanomaterials in cancer-therapy drug delivery system. *Journal of Biomedical Nanotechnology* vol. 9 Preprint at https://doi.org/10.1166/jbn.2013.1583 (2013).

39. Corbex, M., Burton, R. & Sancho-Garnier, H. Breast cancer early detection methods for low and middle income countries, a review of the evidence. *Breast* vol. 21 428–434 Preprint at https://doi.org/10.1016/j.breast.2012.01.002 (2012).

40. Suh, Y. J., Jung, J. & Cho, B. J. Automated breast cancer detection in digital mammograms of various densities via deep learning. *J Pers Med* **10**, (2020).

41. Morrow, M., Waters, J. & Morris, E. MRI for breast cancer screening, diagnosis, and treatment. *The Lancet* **378**, 1804–1811 (2011).

42. Drukker, K., Giger, M. L., Vyborny, C. J. & Mendelson, E. B. Computerized detection and classification of cancer on breast ultrasound1. *Acad Radiol* **11**, 526–535 (2004).

43. Barba, D. *et al.* Breast cancer, screening and diagnostic tools: All you need to know. *Crit Rev Oncol Hematol* **157**, 103174 (2021).

44. Seoane, J. & de Mattos-Arruda, L. The challenge of intratumour heterogeneity in precision medicine. *J Intern Med* **276**, (2014).

45. Magnoni, F. *et al.* Breast cancer surgery: New issues. *Current Oncology* vol. 28 Preprint at https://doi.org/10.3390/curroncol28050344 (2021).

46. Neugut, A. I. *et al.* Increased risk of lung cancer after breast cancer radiation therapy in cigarette smokers. *Cancer* **73**, (1994).

47. Wengström, Y. *et al.* Optitrain: A randomised controlled exercise trial for women with breast cancer undergoing chemotherapy. *BMC Cancer* **17**, (2017).

48. Delort, L. *et al.* Hormonal therapy resistance and breast cancer: Involvement of adipocytes and leptin. *Nutrients* **11**, (2019).

49. Jiang, N. *et al.* Novel treatment strategies for patients with HER2-positive breast cancer who do not benefit from current targeted therapy drugs (Review). *Experimental and Therapeutic Medicine* vol. 16 Preprint at https://doi.org/10.3892/etm.2018.6459 (2018).

50. Rella, R. *et al.* Background parenchymal enhancement in breast magnetic resonance imaging: A review of current evidences and future trends. *Diagnostic and Interventional Imaging* vol. 99 815–826 Preprint at https://doi.org/10.1016/j.diii.2018.08.011 (2018).

51. Nguyen, Q. D., Tenreiro, A., Roberts, J. T., Tavana, A. & Robinson, A. S. Hematoma Mimicking Breast Cancer on CT Scan and Breast Ultrasound. *Cureus* (2020) doi:10.7759/cureus.9099.

52. Langer, J. *et al.* Present and future of surface-enhanced Raman scattering. *ACS Nano* vol. 14 Preprint at https://doi.org/10.1021/acsnano.9b04224 (2020).

53. Heidrich, I., Ačkar, L., Mossahebi Mohammadi, P. & Pantel, K. Liquid biopsies: Potential and challenges. *International Journal of Cancer* vol. 148 Preprint at https://doi.org/10.1002/ijc.33217 (2021).

54. Neumann, M. H. D., Bender, S., Krahn, T. & Schlange, T. ctDNA and CTCs in Liquid Biopsy – Current Status and Where We Need to Progress. *Computational and Structural Biotechnology Journal* vol. 16 Preprint at https://doi.org/10.1016/j.csbj.2018.05.002 (2018).

55. Honoré, N., Galot, R., van Marcke, C., Limaye, N. & Machiels, J. P. Liquid biopsy to detect minimal residual disease: Methodology and impact. *Cancers* vol. 13 Preprint at https://doi.org/10.3390/cancers13215364 (2021).

56. Guitynavard, F., Azadvari, M., Reis, L. O. & Sheikh, M. Liquid biopsy in bladder tumors. in *Liquid Biopsy in Urogenital Cancers and its Clinical Utility* (2022). doi:10.1016/B978-0-323-99884-0.00008-2.

57. Yee, N. S. Liquid biopsy: A biomarker-driven tool towards precision oncology. *Journal of Clinical Medicine* vol. 9 Preprint at https://doi.org/10.3390/jcm9082556 (2020).

58. Burklund, A., Tadimety, A., Nie, Y., Hao, N. & Zhang, J. X. J. Advances in diagnostic microfluidics. in *Advances in Clinical Chemistry* vol. 95 (2020).

59. McBride, J. D. *et al.* Proteomic analysis of bone marrow-derived mesenchymal stem cell extracellular vesicles from healthy donors: implications for proliferation, angiogenesis, Wnt signaling, and the basement membrane. *Stem Cell Res Ther* **12**, (2021).

60. Lin, C., Liu, X., Zheng, B., Ke, R. & Tzeng, C. M. Liquid biopsy, ctDNA diagnosis through NGS. *Life* vol. 11 Preprint at https://doi.org/10.3390/life11090890 (2021).

61. Pessoa, L. S., Heringer, M. & Ferrer, V. P. ctDNA as a cancer biomarker: A broad overview. *Critical Reviews in Oncology/Hematology* vol. 155 Preprint at https://doi.org/10.1016/j.critrevonc.2020.103109 (2020).

62. Alix-Panabières, C. & Pantel, K. Clinical applications of circulating tumor cells and circulating tumor DNA as liquid biopsy. *Cancer Discovery* vol. 6 479–491 Preprint at https://doi.org/10.1158/2159-8290.CD-15-1483 (2016).

63. Abou Daya, S. & Mahfouz, R. Circulating tumor DNA, liquid biopsy, and next generation sequencing: A comprehensive technical and clinical applications review. *Meta Gene* vol. 17 Preprint at https://doi.org/10.1016/j.mgene.2018.06.013 (2018).

64. Aravanis, A. M., Lee, M. & Klausner, R. D. Next-Generation Sequencing of Circulating Tumor DNA for Early Cancer Detection. *Cell* vol. 168 Preprint at https://doi.org/10.1016/j.cell.2017.01.030 (2017).

65. Wan, J. C. M. *et al.* Liquid biopsies come of age: Towards implementation of circulating tumour DNA. *Nature Reviews Cancer* vol. 17 Preprint at https://doi.org/10.1038/nrc.2017.7 (2017).

66. Clatot, F. Review ctDNA and Breast Cancer. in *Recent Results in Cancer Research* vol. 215 (2020).

67. Campos, C. D. M. *et al.* Microfluidic-based solid phase extraction of cell free DNA. *Lab Chip* **18**, (2018).

68. Sorber, L. *et al.* A Comparison of Cell-Free DNA Isolation Kits: Isolation and Quantification of Cell-Free DNA in Plasma. *Journal of Molecular Diagnostics* **19**, (2017).

69. Moore, D. & Dowhan, D. Purification and concentration of DNA from aqueous solutions. *Current protocols in molecular biology / edited by Frederick M. Ausubel ... [et al.]* **Chapter 2**, (2002).

70. Carvalho, J. *et al.* Highly efficient DNA extraction and purification from olive oil on a washable and reusable miniaturized device. *Anal Chim Acta* **1020**, (2018).

71. Carvalho, J. *et al.* Single-use microfluidic device for purification and concentration of environmental DNA from river water. *Talanta* **226**, (2021).

72. Mauger, F., Dulary, C., Daviaud, C., Deleuze, J. F. & Tost, J. Comprehensive evaluation of methods to isolate, quantify, and characterize circulating cell-free DNA from small volumes of plasma. *Anal Bioanal Chem* **407**, (2015).

73. Volpatti, L. R. & Yetisen, A. K. Commercialization of microfluidic devices. *Trends in Biotechnology* vol. 32 Preprint at https://doi.org/10.1016/j.tibtech.2014.04.010 (2014).

74. Lee, H. H., Smoot, J., McMurray, Z., Stahl, D. A. & Yager, P. Recirculating flow accelerates DNA microarray hybridization in a microfluidic device. *Lab Chip* **6**, (2006).

75. Lin, B. *et al.* Microfluidic-Based Exosome Analysis for Liquid Biopsy. *Small Methods* vol. 5 Preprint at https://doi.org/10.1002/smtd.202001131 (2021).

76. Chen, C. *et al.* Microfluidic isolation and transcriptome analysis of serum microvesicles. *Lab Chip* **10**, (2010).

77. Kanwar, S. S., Dunlay, C. J., Simeone, D. M. & Nagrath, S. Microfluidic device (ExoChip) for on-chip isolation, quantification and characterization of circulating exosomes. *Lab Chip* **14**, (2014).

78. Zhao, Z., Yang, Y., Zeng, Y. & He, M. A microfluidic ExoSearch chip for multiplexed exosome detection towards blood-based ovarian cancer diagnosis. *Lab Chip* **16**, (2016).

79. Descamps, L., Roy, D. le & Deman, A. L. Microfluidic-Based Technologies for CTC Isolation: A Review of 10 Years of Intense Efforts towards Liquid Biopsy. *International Journal of Molecular Sciences* vol. 23 Preprint at https://doi.org/10.3390/ijms23041981 (2022).

80. Cady, N. C., Stelick, S. & Batt, C. A. Nucleic acid purification using microfabricated silicon structures. *Biosens Bioelectron* **19**, 59–66 (2003).

81. Hindson, B. J. *et al.* Development of an automated DNA purification module using a micro-fabricated pillar chip. *Analyst* **133**, 248–255 (2008).

82. Cao, W., Easley, C. J., Ferrance, J. P. & Landers, J. P. Chitosan as a polymer for pH-induced DNA capture in a totally aqueous system. *Anal Chem* **78**, 7222–7228 (2006).

83. Campos, C. D. M. *et al.* Microfluidic-based solid phase extraction of cell free DNA. *Lab Chip* **18**, 3459–3470 (2018).

84. Errando-Herranz, C. *et al.* MEMS for Photonic Integrated Circuits. *IEEE Journal of Selected Topics in Quantum Electronics* **26**, (2020).

85. Toropov, N. & Vartanyan, T. Noble metal nanoparticles: Synthesis and optical properties. in *Comprehensive Nanoscience and Nanotechnology* vols 1–5 (2019).

86. van Rossum, M. Integrated Circuits. *Encyclopedia of Condensed Matter Physics* 394–403 (2005) doi:10.1016/B0-12-369401-9/00503-9.

87. Xia, Y. & Whitesides, G. M. Soft lithography. *Annual Review of Materials Science* **28**, (1998).

88. Riedel, D. & Mizaikoff, B. Surface Imprinted Micro- and Nanoparticles. in *Comprehensive Analytical Chemistry* vol. 86 (2019).

89. Ahmad, Z. & Rahman, A. M. N. A. A. Plastics in Waveguide Application. in *Encyclopedia of Materials: Plastics and Polymers* (2022). doi:10.1016/b978-0-12-820352-1.00163-2.